Title

Dynamics of Fungal and Bacterial Biomass Carbon in Natural Ecosystems: Site-Level Applications of the CLM-Microbe Model

Journal

Journal of Advances in Modeling Earth Systems, 13(2)

ISSN

1942-2466

Authors

He, Liyuan
Lipson, David A
Rodrigues, Jorge L Mazza
et al.

Publication Date

2021-02-01

DOI

10.1029/2020ms002283

Peer reviewed

JAMES | Journal of Advances in Modeling Earth Systems

RESEARCH ARTICLE
10.1029/2020MS002283

Dynamics of Fungal and Bacterial Biomass Carbon in Natural Ecosystems: Site-Level Applications of the CLM-Microbe Model

Liyuan He[1], David A. Lipson[1], Jorge L. Mazza Rodrigues[2], Melanie Mayes[3], Robert G. Björk[4,5], Bruno Glaser[6], Peter Thornton[3], and Xiaofeng Xu[1]

[1]Biology Department, San Diego State University, San Diego, CA, USA, [2]Department of Land, Air and Water Resources, University of California-Davis, Davis, CA, USA, [3]Climate Change Science Institute and Environmental Sciences Division, Oak Ridge National Laboratory, Oak Ridge, TN, USA, [4]Department of Earth Sciences, University of Gothenburg, Gothenburg, Sweden, [5]Gothenburg Global Biodiversity Centre, Gothenburg, Sweden, [6]Soil Biogeochemistry, Institute of Agricultural and Nutritional Sciences, Martin Luther University Halle-Wittenberg, Halle (Saale), Germany

Key Points:

- We carried out the site-level parameterization and validation of CLM-Microbe
- The CLM-Microbe model is able to reasonably capture the seasonal dynamics of fungal and bacterial biomass C
- Microbial turnover rate, C:N ratio, and microbial assimilation efficiency are key parameters controlling microbial roles on C cycling

Correspondence to:
X. Xu,
xxu@sdsu.edu

Citation:
He, L., Lipson, D. A., Mazza Rodrigues, J. L., Mayes, M., Björk, R. G., Glaser, B., et al. (2020). Dynamics of fungal and bacterial biomass carbon in natural ecosystems: Site-level applications of the CLM-Microbe model. *Journal of Advances in Modeling Earth Systems*, *12*, e2020MS002283. https://doi.org/10.1029/2020MS002283

Received 10 AUG 2020
Accepted 3 DEC 2020

Abstract Explicitly representing microbial processes has been recognized as a key improvement to Earth system models for the realistic projections of soil carbon (C) and climate dynamics. The CLM-Microbe model builds upon the CLM4.5 and explicitly represents two major soil microbial groups, fungi and bacteria. Based on the compiled time-series data of fungal (FBC) and bacterial (BBC) biomass C from nine biomes, we parameterized and validated the CLM-Microbe model, and further conducted sensitivity analysis and uncertainty analysis for simulating C cycling. The model performance was evaluated with mean absolute error (MAE), root mean square error (RMSE), and coefficient of determination (R^2) for relative change in FBC and BBC. The CLM-Microbe model is able to reasonably capture the seasonal dynamics of FBC and BBC across biomes, particularly for tropical/subtropical forest, temperate broadleaf forest, and grassland, with MAE <0.49 for FBC and <0.36 for BBC and RMSE <0.52 FBC and <0.39 for BBC, while R^2 values are relatively smaller in some biomes (e.g., shrub) due to small sample sizes. We found good consistencies between simulated and observed FBC ($R^2 = 0.70$, $P < 0.001$) and BBC ($R^2 = 0.26$, $P < 0.05$) on average across biomes, but the model is not able to fully capture the large variation in observed FBC and BBC. Sensitivity analysis shows the most critical parameters are turnover rate, carbon-to-nitrogen ratio of fungi and bacteria, and microbial assimilation efficiency. This study confirms that the explicit representation of soil microbial mechanisms enhances model performance in simulating C variables such as heterotrophic respiration and soil organic C density. The further application of the CLM-Microbe model would deepen our understanding of microbial contributions to the global C cycle.

1. Introduction

Global climate change is primarily caused by human-induced increases in atmospheric greenhouse gases, modulated by terrestrial ecosystems through a multitude of climate-ecosystem feedbacks (Gruber & Galloway, 2008; Keohane, 2015; Peters et al., 2012; Zaehle et al., 2010). Heterotrophic respiration, the second largest carbon (C) flux in terrestrial ecosystems, is primarily driven by soil microbes (Gougoulias et al., 2014; Sulman et al., 2014; Van Der Heijden et al., 2018). Although progress has been made in understanding how microbes affect C cycling, more research is needed on accurately projecting microbial feedbacks to the climate change. Large uncertainties in global C projections challenge the current model framework (Luo et al., 2015; Taylor et al., 2011), and the implicit representation of soil microbes may partially reduce those uncertainties (Fang et al., 2005; Wieder et al., 2013, 2015; Xu et al., 2014).

The importance of soil microbes in governing the terrestrial C cycle has received growing attention, and soil microbial processes have been implicitly represented in ecosystem models (Schimel & Weintraub, 2003; Treseder et al., 2012). The development of soil microbial models, such as the SCAMPS model (Sistla et al., 2014), DAMM model (Davidson et al., 2012), microbial-enzyme model (Allison et al., 2010), and MEND model (G. Wang et al., 2013), proved to be valuable in simulating microbial feedbacks to soil C processes. Soil microbial traits such as enzyme production, temperature sensitivity, carbon use efficiency (CUE), microbial and abiotic interaction, and priming effects were incorporated into soil microbial models

(Allison, 2012; Allison et al., 2010; Tang & Riley, 2015). Recently, soil microbes and microbial traits have increasingly been incorporated into Earth system models (ESMs) (Sulman et al., 2014). However, these models assumed that biological responses of soil microbial community are functionally equivalent and exert invariant effects on soil processes (Bradford & Fierer, 2012). Given the large temporal variations in soil microbial community (Cleveland et al., 2007; Díaz-Raviña et al., 1995; Lipson et al., 2002; Lipson & Schmidt, 2004), the assumption of a static soil microbial community is increasingly questioned (G. Wang et al., 2015; Wieder et al., 2014, 2015).

Developing models that explicitly represent soil microbial processes poses an important challenge for ESMs. Recently, the classification of soil microbes in the TRIPLEX-Microbe model (active and dormant components) and the MIMICS model (K- and r-strategists) advanced the representation of the soil microbial community and its functions in ESMs (K. Wang et al., 2017; Wieder et al., 2014). However, the distinct roles of broad soil microbial groups (e.g., fungi and bacteria) have not yet been considered in models. Bacteria and fungi have different physiological traits, for example, bacteria prefer to decompose litter low in carbon-to-nitrogen (C:N) ratio, while fungi tend to decompose litter with higher C:N ratio (Paul, 2016). These differences may cause considerable distinct trajectories of C responses to changing environments such as atmospheric nitrogen (N) deposition, elevated carbon dioxide (CO_2), and precipitation change (Bell et al., 2014; Hopkins et al., 2006; Rousk & Bååth, 2011; Strickland & Rousk, 2010). The classification of the soil microbial community into K- and r-strategists based on functional traits improves the representation of distinct roles of soil microbial groups in biogeochemical processes; however, this characterization is largely theoretical and may therefore limit the effort of directly applying observational data to constrain the microbial parameters.

Fungi and bacteria, two major measurable soil microbial groups playing distinct roles on soil processes, comprise over 90% of the total soil microbial biomass and are the major agents responsible for soil organic matter mineralization (Beare, 1997). Although fungi are widely believed to decompose low quality compounds such as lignin, bacterial ligninases are also commonly found, both fungi and bacteria decompose plant residues and soil organic matter (Burns et al., 2013). For example, as litter quality decreases, fungi are expected to play more important roles (Van Der Heijden et al., 2018). Soil fungal and bacterial biomass are important components of soil microbial community (L. He et al., 2020), representing the microbial ability to conduct biochemical transformation of C and nutrients (Xu et al., 2013). Therefore, variations in fungal:bacterial (F:B) biomass ratio can imply changes in the population of decomposers as well as changes in soil microbial community composition and function (Six et al., 2006).

To fill the research gap of explicitly representing soil microbial community functions in ESMs, we developed the CLM-Microbe model based on the framework in Xu et al. (2014). Fungi- and bacteria-regulated processes such as the decomposition of plant and microbial residues were added into the CLM4.5 to mechanistically represent major soil microbial processes (Figure 1). To distinguish the physiological traits of fungi and bacteria in soil processes, different parameters for fungal- and bacterial-regulated processes were developed and tested. In this study, we reported the model parameterization, sensitivity analysis, and uncertainty analysis at the site level for nine different biomes, and further analyzed the simulated dynamics of microbial biomass carbon and their controls. The key objectives were to: (1) parameterize the CLM-Microbe model using observed time-series data of fungal (FBC) and bacterial (BBC) biomass C in diverse biomes, (2) evaluate the performance of the CLM-Microbe model in simulating FBC and BBC dynamics, and (3) identify the key parameters and processes controlling variations in FBC and BBC.

2. Methodology

2.1. Data Sources

Due to the large variation in soil microbial community among biomes, we parameterized the model by biome (Xu et al., 2014). We selected time-series observed data of FBC and BBC from nine natural biomes (i.e., tropical/subtropical forest, temperate coniferous forest, temperate broadleaf forest, boreal forest, shrub, grassland, desert, tundra, and wetland), with at least two sites in each biome. Then, we randomly selected one site for model calibration and the others for model validation. Finally, nine sites were used for model calibration and 12 sites for model validation for nine natural biomes. Site information, including geographic location, biome type, site name, site ID, sampling years, and the measurement methods, was presented in Table 1.

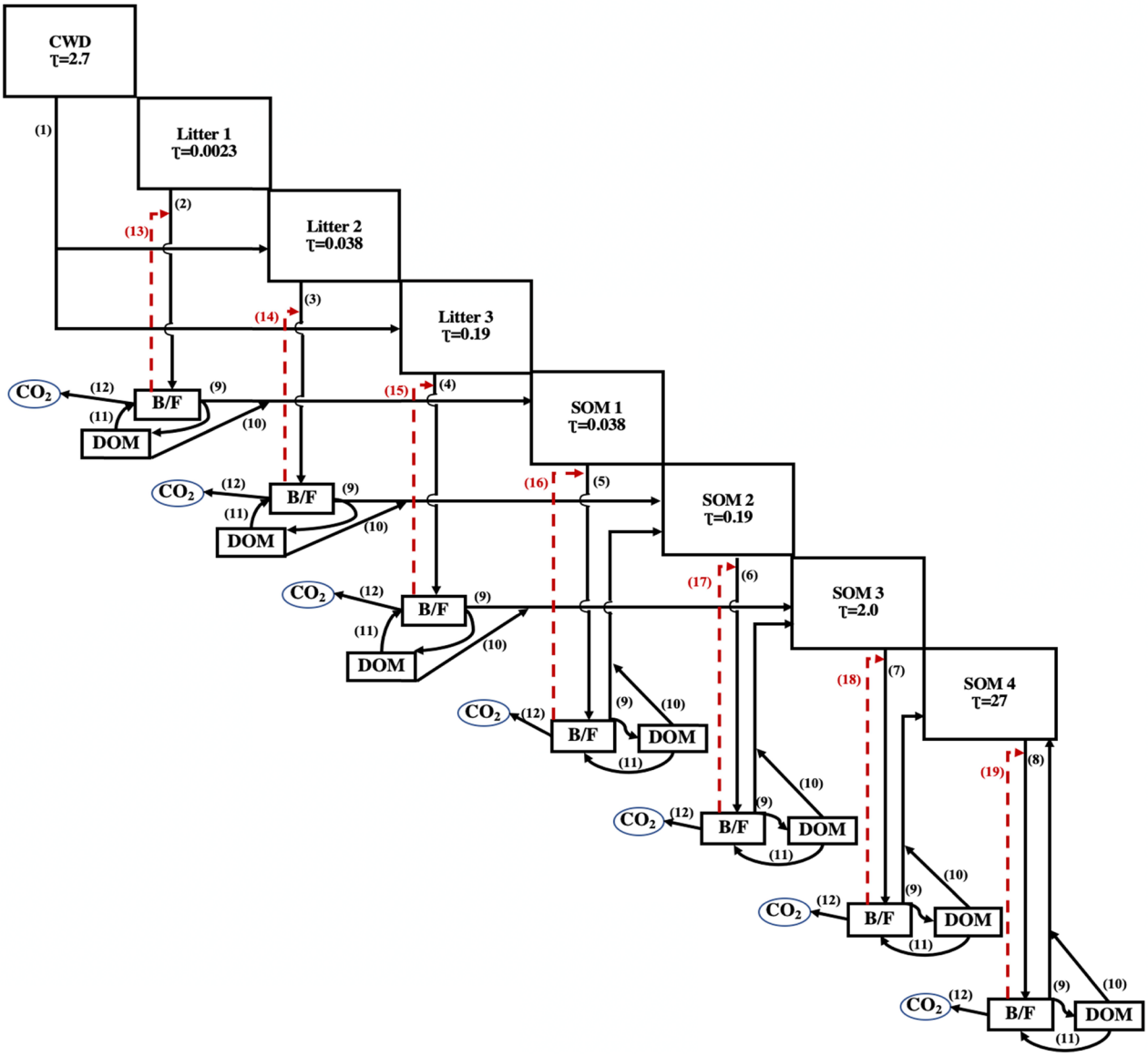

Figure 1. Conceptual diagram showing the key processes and the roles of fungi and bacteria in the CLM-Microbe model. CWD, coarse woody debris; SOM, soil organic matter; B, bacteria; F, fungi; DOM, dissolved organic matter. In the CLM-Microbe model, number in the box means turnover time of each pool. Black solid lines indicate transitions in the CLM-Microbe model, which generally represents processes such as: (1) decomposition of coarse woody debris, (2) litter 1 decomposition, (3) litter 2 decomposition, (4) litter 3 decomposition, (5) soil organic matter 1 decomposition, (6) soil organic matter 2 decomposition, (7) soil organic matter 3 decomposition, (8) soil organic matter 4 decomposition, (9) fungal and bacterial lysis, (10) dissolved organic matter decomposition, (11) dissolved organic matter uptake by fungal and bacterial, and (12) fungal and bacterial respiration. Red dash lines represent regulatory role of fungi and bacteria on the process, including fungi and bacteria regulation on (13) litter 1, (14) litter 2, (15) litter 3, (16) soil organic matter 1, (17) soil organic matter 2, (18) soil organic matter 3, and (19) soil organic matter 4 decomposition.

The FBC and BBC were derived from multiple approaches, such as direct microscopy using optical microscope (DMO) or fluorescence microscope (DMF), plate count (PC), chloroform fumigation (CF), fatty acid methyl ester (FAME), and phospholipid fatty acid (PLFA). Based on our previous study, large variations exist in measured fungal and bacterial biomass among different approaches (L. He et al., 2020). The PLFA was the most widely used in field observed data (Table 2), and likely the most appropriate approach for estimating FBC and BBC simultaneously (L. He et al., 2020; Waring et al., 2013). To reduce the biases introduced by various approaches, we converted the reported FBC and BBC measured using DMO (Balser et al., 2005; Olsson & Wallander, 1998), DMF (Frostegård & Bååth, 1996; Stahl & Parkin, 1996), PC (Bai

Table 1
Site Information of the Observational Data

Phase	Biome	Site ID	Location	Country	Measurement	Depth (cm)	Sampling year	Reference
Calibration	Tropical/subtropical forest	TSF-HS	22.57°N, 112.83°E	China	PLFA	0–10	2012–2014	Zhao et al. (2017)
	Temperate coniferous forest	TCF-NJ	39.92°N, 74.6°W	US	PLFA	0–2.3	2006–2008	Landesman and Dighton (2010)
	Temperate broadleaf forest	TBF-VA	48.21°N, 16.36°E	Austria	PLFA	0–5	2006–2008	Kaiser et al. (2010)
	Boreal forest	BRF-WC	65.32°N, 142.31°W	US	DMO	5–20	1973	Flanagan and Van Cleve (1977)
	Shrub	SHB-OB	40.18°N, 112.46°W	US	PLFA & FAME	0–10	2009–2010	Docherty et al. (2015)
	Grassland	GRS-IA	42.18°N, 93.5°W	US	DMO	0–10	2001–2002	Dornbush et al. (2008)
	Desert	DST-CH	29.08°N, 103.17°W	US	CF & FAME	0–15	2004–2006	Bell et al. (2014)
	Tundra	TUN-MH	68.36°N, 18.50°E	Sweden	PLFA	0–10	2006	Björk et al. (2008)
	Wetland	WET-EM	51.91°N, 11.98°E	Germany	PLFA	0–20	1999–2000	Moche et al. (2015)
Validation	Tundra	TUN-ES	64.83°N, 111.63°W	Canada	DMF	0–5	2007	Buckeridge et al. (2013)
	Temperate coniferous forest	TCF-NT	47.58°N, 11.64°E	Australia	PLFA	0–5	2008–2009	Schindlbacher et al. (2011)
	Desert	DST-GB	44.28°N, 87.93°E	China	PLFA	0–5	2011–2013	Huang et al. (2015)
	Desert	DST-JN	32.59°N, 106.84°W	US	PLFA	0–30	2017	National Ecological Observatory Network (2020)
	Boreal forest	BRF-AL	65.15°N, 147.5°W	US	PLFA & FAME	0–10	2009	Docherty et al. (2015)
	Tropical/subtropical forest	TSF-OS	29.69°N, 81.99°W	US	PLFA & FAME	0–10	2009–2010	Docherty et al. (2015)
	Grassland	GRS-BC	49.23°N, 121.77°W	Canada	DMO	0–10	1997–1999	Bittman et al. (2005)
	Temperate broadleaf forest	TBF-SH	36.02°N, 106.47°E	China	PLFA	0–11	2012–2013	Liu et al. (2018)
	Temperate broadleaf forest	TBF-MS	37.38°N, 80.52°W	US	PLFA	0–30	2018	National Ecological Observatory Network (2020)
	Temperate broadleaf forest	TBF-TL	32.95°N, 87.39°W	US	PLFA	0–30	2017	National Ecological Observatory Network (2020)
	Shrub	SHB-AC	30.63°S, 71.67°W	Chile	CFU	0–20	1997–2006	Aguilera et al. (2016)
	Wetland	WET-EF	51.87°N, 12.39°E	Germany	PLFA	0–20	1998–2000	Moche et al. (2015)

Abbreviations: CF, chloroform fumigation; DMF, direct count using fluorescence microscope; DMO, direct microscopy using optical microscope; FAME, fatty acid methyl ester; PC, plate count; PLFA, phospholipid fatty acid.

et al., 2013; Priha et al., 1999), CF (Bailey et al., 2002), and FAME (Miura et al., 2017) to PLFA measured values using the conversion factors reported by previous studies (Frostegård & Bååth, 1996; Klamer & Bååth, 2004).

2.2. Model Improvements

The CLM-Microbe model was developed based on the default CLM4.5 with vertical profiles of biogeochemistry, and we specifically incorporated soil microbial processes into the decomposition subroutines (Koven

Table 2
Key Model Parameters in Processes Involving Fungal and Bacterial Biomass

Symbol	Range[a]	Unit	Description	Reference
k_dom	0.0025–0.5	d^{-1}	Decomposition rate constant of DOM	Cherrier et al. (1996), Kirchman et al. (1991), Wheeler et al. (1996)
k_bacteria	0.00143–2	d^{-1}	Lysis rate constant of bacteria	Moore et al. (2005), Rousk and Bååth (2007, 2011), Schippers et al. (2005)
k_fungi	0.00027–0.05	d^{-1}	Lysis rate constant of fungi	Moore et al. (2005), Rousk and Bååth (2011), Thornton and Rosenbloom (2005), Wallander et al. (2004)
m_rf_s1m	0–1		Fraction factor quantifying carbon from SOM1 to microbes	Calibrated
m_rf_s2m	0–1		Fraction factor quantifying carbon from SOM2 to microbes	Calibrated
m_rf_s3m	0–1		Fraction factor quantifying carbon from SOM3 to microbes	Calibrated
m_rf_s4m	0–1		Fraction factor quantifying carbon from SOM4 to microbes	Calibrated
m_batm_f	0–1		Fraction factor quantifying carbon respired by bacteria	Calibrated
m_bdom_f	0–1		Fraction factor quantifying carbon from DOM to bacteria	Calibrated
m_bs1_f	0–1		Fraction factor quantifying carbon from bacteria to SOM1	Calibrated
m_bs2_f	0–1		Fraction factor quantifying carbon from bacteria to SOM2	Calibrated
m_bs3_f	0–1		Fraction factor quantifying carbon from bacteria to SOM3	Calibrated
m_fatm_f	0–1		Fraction factor quantifying carbon respired by fungi	Calibrated
m_fdom_f	0–1		Fraction factor quantifying carbon from DOM to fungi	Calibrated
m_fs1_f	0–1		Fraction factor quantifying carbon from fungi to SOM1	Calibrated
m_fs2_f	0–1		Fraction factor quantifying carbon from fungi to SOM2	Calibrated
m_fs3_f	0–1		Fraction factor quantifying carbon from fungi to SOM3	Calibrated
m_domb_f	0–1		Fraction factor quantifying carbon from DOM to bacteria	Calibrated
m_domf_f	0–1		Fraction factor quantifying carbon from DOM to fungi	Calibrated
m_doms1_f	0–1		Fraction factor quantifying carbon from DOM to SOM1	Calibrated
m_doms2_f	0–1		Fraction factor quantifying carbon from DOM to SOM2	Calibrated
m_doms3_f	0–1		Fraction factor quantifying carbon from DOM to SOM3	Calibrated
cn_bacteria	3–12		C:N ratio of bacteria	Strickland and Rousk, (2010)
cn_fungi	3–60		C:N ratio of fungi	Strickland and Rousk (2010)
cn_dom	4.2–185		C:N ratio of DOM	Sinsabaugh et al. (2016)
CUEmax	0.46–0.9		Maximum carbon use efficiency of microbes	Gommers et al. (1988), Sinsabaugh et al. (2013, 2016)

Abbreviation: CUE, carbon use efficiency.
[a]The values may not be the same as those from literature sources due to unit conversion.

et al., 2013; Thornton et al., 2007; Thornton & Rosenbloom, 2005). The key algorithm for simulating microbial controls on C processes is based on the model framework in Xu et al. (2014). The CLM4.5 classified litter into three pools, that is, litter 1 (labile), litter 2 (cellulose), and litter 3 (lignin), and soil organic matter (SOM) into four pools, that is, SOM 1, SOM 2, SOM 3, and SOM 4. The three litter and four SOM pools differ in base decomposition rate (τ), with turnover time of litter pools ranging from 20 h to 71 days and SOM pools ranging from 14 days to 27 years (Figure 1). Coarse woody debris is fragmented, decomposed, and gradually transferred into litter pools, and further from litter to SOM pools (Koven et al., 2013).

One critical improvement in the CLM-Microbe model is the representation of the pools of dissolved organic matter (DOM), fungal and bacterial biomass into the biogeochemistry cascade in the default CLM4.5 (Figure 1). The DOM pool is further linked with a microbial functional group-based methane module (Y. Wang et al., 2019; Xu et al., 2015). In the decomposition subroutine, we changed the original transfers from litter

to SOM to mechanisms that were mediated by soil fungi and bacteria. Specifically, we added the C transfer from litter and SOM pools to fungal and bacterial biomass pools and DOM, from DOM pool to fungal and bacterial biomass and SOM pools, and from fungal and bacterial biomass pools to DOM and SOM pools. A certain proportion of C, defined by fraction factors in fungal and bacterial biomass pools, will be respired as CO_2 into the atmosphere. In total, the CLM-Microbe model included 41 transitions mediated by fungi and bacteria, which largely increased the accuracy of simulating the complex soil processes relative to nine transitions in the default CLM4.5. In each soil layer, these transitions are regulated by environmental factors (e.g., temperature, moisture, and oxygen) in the soil. We defined 26 parameters related to fungi and bacteria related processes in the CLM-Microbe model, with the range and description of each parameter to be found in Table 2. The code for the CLM-Microbe model has been archived at https://github.com/email-clm/clm-microbe, since 2015. The model version used in this study was checked out from GitHub on June 18, 2018.

2.2.1. Vegetation Effects on Soil Microbial Community

Vegetation also has a significant influence on soil microbial growth through litter input and root exudation (Blagodatskaya & Kuzyakov, 2008). Labile C from litter and root exudates, in the form of DOM, can be readily used to enhance fungal and bacterial growth (Göttlicher et al., 2006). Therefore, in addition to the slow breakdown of SOM and litter, the DOM pool is refreshed by a rapid release from living roots and fresh litter, playing an important role in soil microbial activity (Sulman et al., 2014). In the CLM-Microbe model, we incorporated the DOM input from fine roots and litter, and the quantity of DOM input from these pools are determined by a parameter quantifying the labile C release from pools of fine roots and litter and their pool size. The incorporation of DOM input from litter and fine roots represents the vegetation effects on soil microbial community.

2.2.2. Decomposition

The decomposition of SOM, DOM, and litter was controlled by both their potential decomposition rates and environmental conditions. The decomposition processes in the CLM-Microbe model were defined following the equations as below,

$$D_C = k \times r_{\text{oxygen}} \times r_{\text{depth}} \times r_{\text{tsoil}} \times r_{\text{water}}$$

$$r_{\text{depth}} = \exp\left(-\frac{z}{z_\tau}\right)$$

$$r_{\text{tsoil}} = Q_{10}^{\frac{T_{\text{soil,j}} - T_{\text{ref}}}{10}}$$

$$r_{water} = \begin{cases} 0 & for\ \varphi_j < \varphi_{\min} \\ \dfrac{\log\left(\varphi_{\min}/\varphi_j\right)}{\log\left(\varphi_{\min}/\varphi_{\max}\right)} & for\ \varphi_{\min} \le \varphi_j \le \varphi_{\max} \\ 1 & for\ \varphi_j \text{ax} > \varphi_{\text{m}} \end{cases}$$

where D_C is the rate of substrate (e.g., SOM, DOM, and litter) breakdown; k is the potential decomposition rate; r_{oxygen} represents environmental modifier determined by soil oxygen concentration, which is set as 1 for the single layer model; r_{depth} is environmental modifier determined by soil depth, which is set as 1 for the single layer model; r_{water} is environmental modifier determined by soil moisture; r_{tsoil} means environmental modifier determined by soil temperature; z means soil depth; z_τ is the e-folding depth for decomposition; $T_{\text{soil, j}}$ is soil temperature at layer j; T_{ref} is the reference temperature for decomposition, which is set as 25°C; Q_{10} indicates the temperature dependence of decomposition, it is the ratio of the rate at a specific temperature to that at 10°C lower; Ψ_j is the soil water potential in layer j; $\Psi_{\min}$ is a lower limit for soil water potential

Table 3
Key Parameters for the Different Biomes

	Biomes								
Parameters	BRF	DST	GRS	SHB	TBF	TCF	TSF	TUN	WET
m_bdom_f	0.15	0.1	0.15	0.1	0.15	0.15	0.1	0.1	0.08
m_bs1_f	0.1	0.03	0.05	0.05	0.05	0.05	0.03	0.03	0.02
m_bs2_f	0.12	0.06	0.1	0.1	0.1	0.1	0.06	0.06	0.04
m_bs3_f	0.18	0.12	0.15	0.15	0.15	0.15	0.12	0.12	0.08
m_fdom_f	0.15	0.1	0.15	0.1	0.15	0.15	0.1	0.1	0.08
m_fs1_f	0.1	0.03	0.05	0.05	0.05	0.05	0.03	0.03	0.02
m_fs2_f	0.12	0.06	0.1	0.1	0.1	0.1	0.06	0.06	0.04
m_fs3_f	0.18	0.12	0.15	0.15	0.15	0.15	0.12	0.12	0.08
k_dom	0.007	0.007	0.007	0.007	0.008	0.007	0.0005	0.007	0.007
k_bacteria	0.008	0.0178	0.005	0.0036	0.008	0.004	0.0085	0.0032	0.072
k_fungi	0.004	0.009	0.0045	0.002	0.0018	0.002	0.01	0.0012	0.032
m_rf_s1m	0.4	0.4	0.4	0.4	0.4	0.4	0.4	0.4	0.4
m_rf_s2m	0.6	0.6	0.6	0.6	0.6	0.6	0.6	0.6	0.6
m_rf_s3m	0.7	0.7	0.7	0.7	0.7	0.7	0.7	0.7	0.7
m_rf_s4m	0.8	0.8	0.8	0.8	0.8	0.8	0.8	0.8	0.8
m_batm_f	0.2	0.08	0.12	0.08	0.12	0.12	0.12	0.12	0.1
m_fatm_f	0.1	0.04	0.08	0.04	0.08	0.08	0.08	0.08	0.06
m_domb_f	0.008	0.12	0.04	0.16	0.86	0.045	0.05	0.24	0.27
m_domf_f	0.001	0.18	0.9	0.64	0.04	0.005	0.89	0.56	0.45
m_doms1_f	0.32	0.24	0.03	0.1	0.06	0.32	0.03	0.1	0.14
m_doms2_f	0.27	0.2	0.02	0.06	0.03	0.28	0.02	0.06	0.08
m_doms3_f	0.22	0.15	0.01	0.03	0.01	0.2	0.01	0.03	0.04
cn_bacteria	5	4	5	5	6	5	5	4	6
cn_fungi	15	15	15	15	12	15	15	16	12
CUEmax	0.8	0.8	0.8	0.8	0.8	0.8	0.8	0.8	0.8

Abbreviations: BRF, boreal forest; CUE, carbon use efficiency; DST, desert; GRS, grassland; SHB, shrub; TBF, temperate broadleaf forest; TCF, temperate coniferous forest; TSF, tropical/subtropical forest; TUN, tundra; WET, wetland.

control on decomposition rate (set to −10 MPa), r_{water} will be set as 0 if Ψ_j is lower than Ψ_{min}; Ψ_{max} is the upper limit for soil water potential control on decomposition, which equals to the saturated soil matric potential, r_{water} will be set as 1 if Ψ_j is higher than Ψ_{max}; $w_{soil,j}$ means soil water content in layer j.

Although there are variations in Q_{10} of substrate mineralization under various land use types, nutrient concentrations, moisture contents, property of substrates, and temperature gradients for measurement (Fierer et al., 2003; Hopkins et al., 2006; Larionova et al., 2007), the Q_{10} value is confined close to 1.5 at ecosystem-level, which is set as default Q_{10} value in CLM4.5. There is no difference in decomposition between aboveground and belowground substrate, Q_{10} values of the decomposition of three litter pools (Litter 1, Litter 2, and Litter 3) and two less stable SOM pools (SOM 1 and SOM 2) were set as 1.5 in the CLM-Microbe model, which is consistent with the default CLM4.5. Stable SOM in deep soils is believed to have higher Q_{10} value than that in surface soils (Fierer et al., 2003; von Lützow & Kögel-Knabner, 2009), indicating that the decomposition of stable SOM in subsurface soil is more sensitive to temperature change than that in surface soil. Therefore, to differentiate the Q_{10} of SOM decomposition in different soil depths, Q_{10} values of third SOM pool and fourth SOM pool are set as 2 and 2.5, respectively, in the CLM-Microbe model. Due to the simple chemical structure and low activation energy of DOM, Q_{10} value of DOM is expected to be lower than SOM and litter (Davidson & Janssens, 2006). Consequently, we set the Q_{10} value of DOM as 1.25 in the CLM-Microbe model.

Table 4
Site-Level Evaluation of the Goodness-of-Fit Criteria Computed for the Simulated Fungal and Bacterial Biomass Dynamics in the Calibration and Validation Phases

		Fungi			Bacteria		
Phase	Site	MAE	RMSE	R^2	MAE	RMSE	R^2
Calibration	DST-CH	0.45	0.60	0.473	0.56	0.76	0.374
	GRS-IA	0.29	0.34	0.042	0.18	0.21	0.381
	SHB-OB	0.06	0.07	0.005	0.06	0.07	0.299
	TUN-MH	1.16	1.43	0.251	1.04	1.11	0.398
	BRF-WC	0.28	0.37	0.384	0.63	0.69	0.830
	TBF-VA	0.28	0.31	0.157	0.26	0.30	0.217
	TCF-NJ	0.23	0.24	0.066	0.37	0.38	0.067
	TSF-HS	0.19	0.24	0.156	0.14	0.17	0.002
	WET-EM	0.41	0.73	0.59	0.42	0.72	0.63
Validation	DST-GB	0.54	0.65	0.513	0.32	0.33	0.269
	DST-JN	0.14	0.14	--	0.15	0.16	--
	GRS-BC	0.30	0.37	0.010	0.20	0.27	0.046
	SHB-AC	0.73	0.79	0.004	1.18	2.02	0.111
	TUN-ES	0.27	0.33	0.411	0.17	0.19	0.014
	BRF-AL	0.41	0.41	--	0.04	0.04	--
	TBF-TL	0.49	0.52	0.064	0.13	0.16	0.625
	TBF-SH	0.17	0.19	0.092	0.24	0.33	0.183
	TBF-MS	0.29	0.35	0.935	0.36	0.39	0.945
	TCF-NT	0.45	0.56	0.014	0.19	0.20	0.450
	TSF-OS	0.01	0.02	0.980	0.19	0.22	0.520
	WET-EF	0.25	0.31	0.071	0.30	0.37	0.052

Abbreviations: MAE, mean absolute error; RMSE, root mean square error; R^2, R square.

Notes. -- indicates not applicable. MAE and RMSE values indicate the mean error of the model, smaller values represent higher model performance. R^2 values mean the proportion of variation being explained by the mode, higher R^2 values indicate better model performance. Due to the difference in variations of simulated and observed fungal and bacterial biomass and our focus of estimating fungal and bacterial biomass dynamics, we did the evaluation using relative change in fungal and bacterial biomass instead, that is, the difference between simulated/observed fungal/bacterial biomass and the average of simulated/observed fungal/bacterial biomass over the average of simulated/observed fungal/bacterial biomass; R^2 is not suitable for assessing the goodness-of-fit for a small amount of data due to the large bias in small samples.

2.2.3. Microbial Lysis

The microbial biomass turnover is closely associated with the SOM formation, while the contribution of microbial biomass residues to the formation of SOM has been largely underestimated (Liang et al., 2019). However, growing evidence showed that the soil microbial community made a relatively high contribution to soil organic carbon (SOC) due to its large pool size (Xu et al., 2013) and fast turnover rate (Glaser et al., 2004). Sinsabaugh et al. (2016) estimated a global mean biomass turnover time of 67 ± 22 days based on a negative linear relationship between CUE and microbial biomass turnover time, with the mean microbial CUE estimated as 0.25–0.30. Xu et al. (2017) also quantified the microbial biomass turnover time as 23 and 28 days based on the area-weighted global average of the metabolic quotient in soils (1.8 μmol C·mmol microbial biomass $C^{-1}{\cdot}h^{-1}$) and reference metabolic quotient (1.5 μmol C·mmol microbial biomass $C^{-1}{\cdot}h^{-1}$), respectively, from a global microbial metabolic quotient data set. These estimates in soil microbial biomass turnover are generally in the same order and vary slightly; however, the turnover rates of different soil microbial groups (e.g., fungi and bacteria) were distinct and in a wide range of variation, with fungal and bacterial biomass turnover rate reported as 0.00143 to 2 d^{-1} (Moore et al., 2005; Rousk & Bååth, 2007, 2011) and 0.00027 to 0.05 d^{-1} (Moore et al., 2005; Rousk & Bååth, 2011; Strickland & Rousk, 2010; Wallander et al., 2004), respectively.

In addition, bacterial and fungal growth are highly sensitive to environmental conditions, such as soil moisture and temperature. As a result, in the CLM-Microbe model, fungal and bacterial biomass lysis process is mechanistically represented as the interactive effects of lysis rate constant and environmental factors, that is, r_{oxygen}, r_{water}, r_{tsoil}, and r_{depth}, described above.

2.2.4. Soil Microbial Respiration

Bacteria and fungi assimilate DOM, SOM, and litter to form their biomass, and a proportion of the assimilated C is respired (Figure 1). The proportion of C used for fungal and bacterial respiration is determined by the factors indicated in Tables 2 and 3. In addition, heterotrophic respiration (HR) is widely affected by multiple abiotic and biotic factors, such as substrate concentration and availability, soil moisture, and soil temperature (Gomez-Casanovas et al., 2012; Zhang et al., 2013). Therefore, fungal and bacterial respirations in the CLM-Microbe model are defined as the interactive effects of substrate (i.e., DOM, SOM, and litter), fraction factors quantifying C being respired by fungi and bacteria, and environmental factors (i.e., r_{oxygen}, r_{water}, r_{tsoil}, and r_{depth}) regulating the respiration process.

2.2.5. Carbon Use Efficiency

The CUE of soil microbes for three litter pools in the CLM-Microbe model are determined following the equation in Sinsabaugh et al. (2013). In addition, CUE is reported to vary with temperature, showing a coefficient of −0.012 with increasing temperature (Devêvre & Horwáth, 2000; Xu et al., 2014). Therefore, we assumed that CUE decreased compared with the ambient thermal regime of microbes' habitats following the equation as below,

$$\mathrm{CUE} = \left(\mathrm{CUE}_{\max} - CUE_T \times \left(T - T_{CUEref}\right)\right) \times \left(M_{\mathrm{C:N}} / S_{\mathrm{C:N}}\right)^{0.6}$$

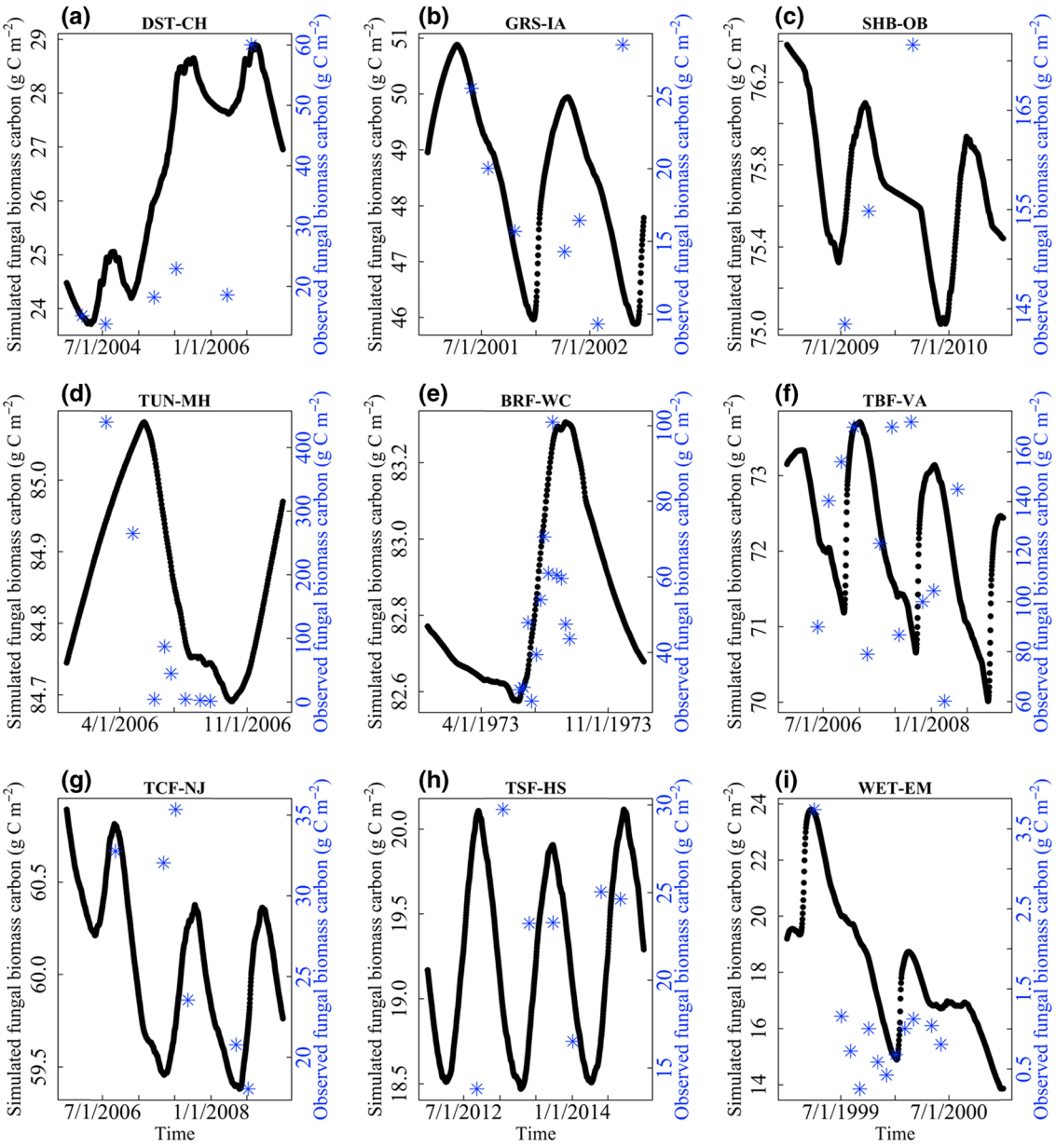

Figure 2. Model calibration of fungal biomass for (a) desert, (b) grassland, (c) shrub, (d) tundra, (e) boreal forest, (f) temperate broadleaf forest, (g) temperate coniferous forest, (h) tropical/subtropical forest, and (i) wetland. The blue star indicates the observed fungal biomass, and the black filled circle represents simulated fungal biomass.

where CUE is C use efficiency, which is defined as the growth-to-assimilation ratio for soil microbes; CUE_{max} is the maximum value of C use efficiency; CUE_T is the coefficient indicating the dependence of C use efficiency on temperature; T_{CUEref} is the reference temperature of C use efficiency, which is defined as 15°C in the CLM-Microbe model; $M_{C:N}$ means the C:N ratio of soil microbial biomass, which is defined as 8 in the CLM-Microbe model; $S_{C:N}$ represents C:N ratio of substrate (e.g., litter).

The C flow from litter and SOM pools to soil microbes will be partitioned by fungal and bacterial biomass pools based on the C:N ratio of fungal and bacterial biomass. The fraction factor quantifying bacteria C gain from litter and SOM is calculated based on the weighted average of assimilation efficiency of fungi and bacteria following the equation as below,

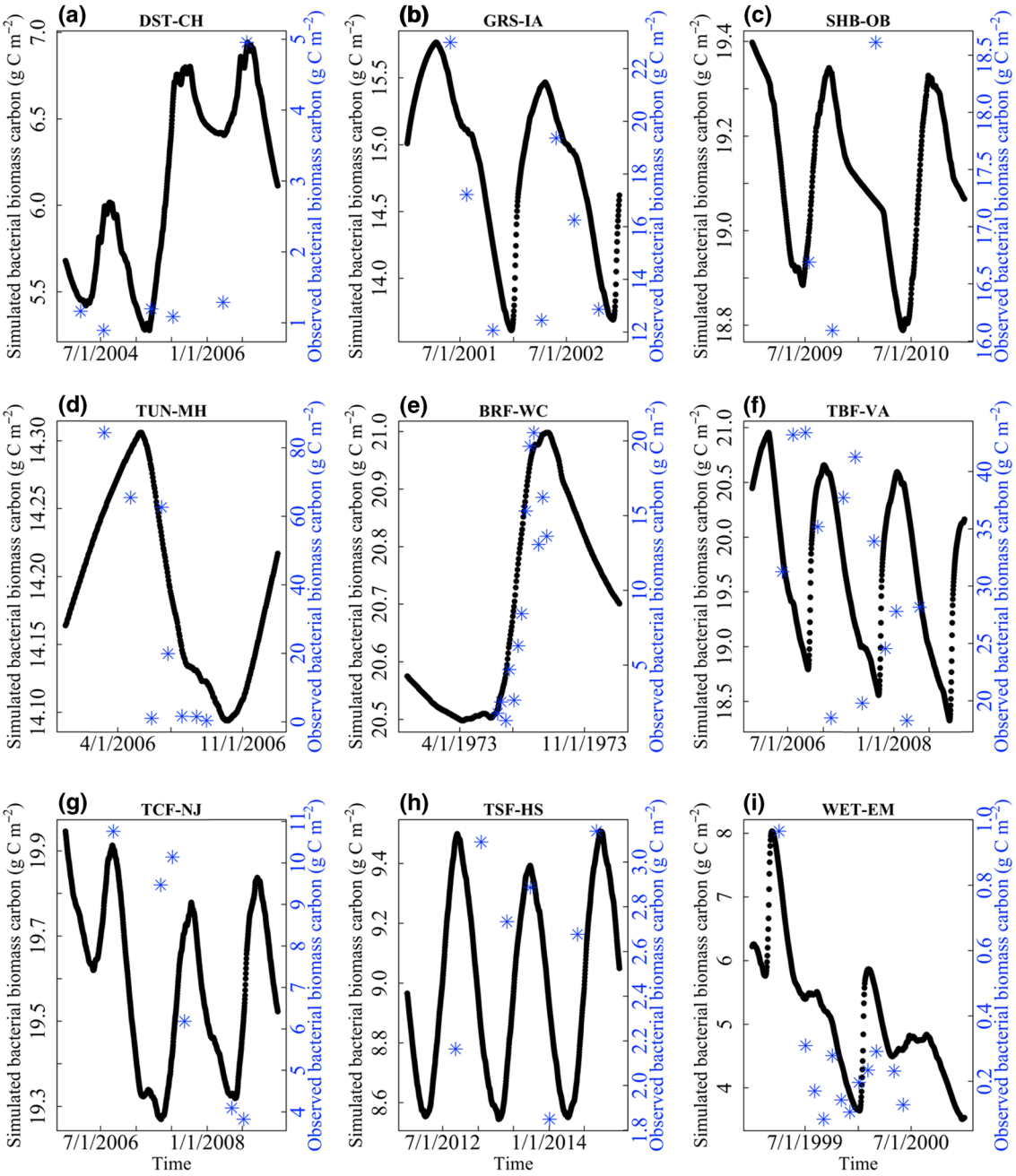

Figure 3. Model calibration of bacterial biomass for (a) desert, (b) grassland, (c) shrub, (d) tundra, (e) boreal forest, (f) temperate broadleaf forest, (g) temperate coniferous forest, (h) tropical/subtropical forest, and (i) wetland. The blue star indicates the observed bacterial biomass, and the black filled circle represents simulated bacterial biomass.

$$fb = \frac{\left(B_{C:N}/S_{C:N}\right)^{0.6}}{\left(F_{C:N}/S_{C:N}\right)^{0.6} + \left(F_{C:N}/S_{C:N}\right)^{0.6}}$$

$$ff = 1 - fb$$

Table 5
Key Parameters Used in Model Sensitivity Analysis and Uncertainty Analysis

Parameters	Ecological meanings
k_dom	Decomposition rate constant of dissolved organic matter
k_bacteria	Lysis rate constant of bacteria
k_fungi	Lysis rate constant of fungi
m_rf_s1m	Fraction factor quantifying carbon from soil organic matter1 to microbes
m_rf_s2m	Fraction factor quantifying carbon from soil organic matter2 to microbes
m_rf_s3m	Fraction factor quantifying carbon from soil organic matter3 to microbes
m_rf_s4m	Fraction factor quantifying carbon from soil organic matter4 to microbes
m_batm_f	Fraction factor quantifying carbon respired by bacteria
m_bdom_f	Fraction factor quantifying carbon from dissolved organic matter to bacteria
m_bs1_f	Fraction factor quantifying carbon from bacteria to soil organic matter1
m_bs2_f	Fraction factor quantifying carbon from bacteria to soil organic matter2
m_bs3_f	Fraction factor quantifying carbon from bacteria to soil organic matter3
m_fatm_f	Fraction factor quantifying carbon respired by fungi
m_fdom_f	Fraction factor quantifying carbon from dissolved organic matter to fungi
m_fs1_f	Fraction factor quantifying carbon from fungi to soil organic matter1
m_fs2_f	Fraction factor quantifying carbon from fungi to soil organic matter2
m_fs3_f	Fraction factor quantifying carbon from fungi to soil organic matter3
m_domb_f	Fraction factor quantifying carbon from dissolved organic matter to bacteria
m_domf_f	Fraction factor quantifying carbon from dissolved organic matter to fungi
m_doms1_f	Fraction factor quantifying carbon from dissolved organic matter to soil organic matter1
m_doms2_f	Fraction factor quantifying carbon from dissolved organic matter to soil organic matter2
m_doms3_f	Fraction factor quantifying carbon from dissolved organic matter to soil organic matter3
cn_bacteria	C:N ratio of bacteria
cn_fungi	C:N ratio of fungi
CUEmax	Maximum carbon use efficiency of microbes

Abbreviation: CUE, carbon use efficiency.

where *fb* is the fraction of C flowing into bacteria; *ff* is the fraction of C flowing into fungi; $B_{C:N}$ means the C:N ratio of BBC; $F_{C:N}$ means the C:N ratio of FBC; $S_{C:N}$ represents C:N ratio of substrates (e.g., litter and SOM).

2.3. Model Forcing Data

The forcing data for this model include meteorological data such as air temperature, relative humidity, incoming solar radiation, longwave radiation, precipitation rate, surface pressure, and surface winds. Since the sampling year of the sites spans from 1973 to 2018, which was not fully covered by any commonly used forcing datasets of CLM. After examining the data distribution, we found that sites sampling later than 2014 are in North America (Table 1). Therefore, for sites sampled before 2014, we extracted the forcing data during January 1, 1971 through December 31, 2014 from CRUNCEP Version 4 provided by Climate Data Gateway at the National Center for Atmospheric Research (https://www.earthsystemgrid.org). The forcing data for sites sampled later than 2014 were extracted from the Global Land Data Assimilation System Version 2 (https://ldas.gsfc.nasa.gov). Using the latitude and longitude information of study sites in each biome (Table 2), we extracted the meteorological variables for all sites. Since the standardized input forcing data are in half-hourly time steps, the extracted 6-hourly data for each study site was interpolated to half-hourly step using linear interpolation via na.approx function in R (R for Mac OS X version 3.5.3).

Table 6
Annual Estimates of Fungal and Bacterial Biomass Carbon, Fungal: Bacterial (F:B) Ratio, Soil Organic Carbon (SOC), and Heterotrophic Respiration (HR) With the Uncertainties of Parameters During the Sampling Years for all Sites

Source	Site/ Biome	Fungal biomass (g C m^{-2})	Bacterial biomass (g C m^{-2})	F:B ratio	SOC (g C m^{-2})	HR (g C m^{-2} yr^{-1})
CLM-Microbe simulated[a]	DST-CH	38.65 (21.69~62.97)	8.90 (5.21~15.17)	4.54 (2.15~7.94)	2567.62 (2011.82~3148.15)	277.41 (269.87~282.88)
	GRS-IA	110.25 (66.94~182.63)	33.57 (21.20~53.26)	3.44 (1.68~5.94)	2677.50 (2225.43~3104.13)	312.85 (307.67~325.92)
	SHB-OB	148.74 (86.44~253.85)	37.33 (22.44~61.57)	4.16 (2.07~7.47)	3363.62 (2908.50~3829.85)	120.69 (117.80~123.25)
	TUN-MH	180.25 (111.67~283.71)	29.89 (19.44~46.77)	6.30 (3.23~10.70)	3603.51 (3460.15~3741.94)	92.75 (90.15~95.48)
	BRF-WC	204.76 (124.98~328.30)	40.10 (27.41~63.30)	5.39 (2.61~9.45)	8685.33 (8133.04~9341.41)	420.07 (367.18~452.30)
	TBF-VA	258.79 (161.16~429.01)	70.47 (45.63~114.71)	3.83 (1.89~6.49)	5872.70 (5221.21~6540.73)	560.48 (538.93~574.73)
	TCF-NJ	379.71 (213.91~683.37)	100.15 (59.46~166.58)	3.96 (1.86~6.95)	7989.60 (6411.33~9961.35)	811.32 (800.71~818.67)
	TSF-HS	37.02 (19.70~62.50)	16.66 (9.11~29.09)	2.31 (1.14~4.19)	2509.49 (1694.83~3422.36)	400.69 (393.76~404.51)
	WET-EM	23.62 (13.52~39.54)	6.63 (4.13~11.03)	3.75 (1.85~6.67)	13203.92 (11732.67~14385.34)	540.32 (524.52~556.59)
CLM4.5 simulated[a]	DST-CH	NA	NA	NA	0.00	0.00
	GRS-IA	NA	NA	NA	11990.54	756.86
	SHB-OB	NA	NA	NA	1598.15	63.07
	TUN-MH	NA	NA	NA	2085.97	94.61
	BRF-WC	NA	NA	NA	3465.00	157.68
	TBF-VA	NA	NA	NA	11238.67	599.18
	TCF-NJ	NA	NA	NA	4920.45	315.36
	TSF-HS	NA	NA	NA	6627.84	536.11
	WET-EM	NA	NA	NA	9950.83	567.65
Observed[b]	DST-CH[d]	24.79 (13.78~60.04)	1.76 (0.89~4.95)	14.05 (12.12~21.13)	NA	NA
	GRS-IA[e]	18.55 (9.32–28.53)	16.17 (12.07–22.99)	1.15 (0.57–2.22)	NA	NA
	SHB-OB[e]	156.65 (143.46–171.62)	17.13 (16.09–18.61)	9.14 (8.60–9.62)	3559.97[e]	NA
	TUN-MH[e]	105.89 (1.10–439.88)	29.63 (0.38–84.42)	3.57 (1.38–5.21)	1945.00[e k]	NA
	BRF-WC[f]	51.71 (27.07–100.96)	9.70 (1.29–20.55)	5.33 (2.92–36.93)	NA	NA
	TBF-VA[g]	122.78 (60.12–171.88)	31.01 (18.30–43.39)	3.96 (2.88–5.15)	NA	NA
	TCF-NJ[h]	27.09 (18.05–35.35)	7.41 (3.82–10.77)	3.65 (3.04–5.08)	NA	NA
	TSF-HS[e]	22.33 (13.81–29.74)	2.65 (1.85–3.14)	8.43 (6.38–9.63)	4238.08[e]	NA
	WET-EM[i]	1.05 (0.25–3.74)	0.26 (0.08–0.97)	4.01 (3.02–6.33)	10819[j]	NA
Biome average[c]	DST	59.04 (14.05–74.00)	15.28 (0.32–60.21)	3.14 (2.20–4.49)	2728.00 (2651.58–2804.42)	NA
	GRS	88.69 (20.55–132.48)	46.14 (2.34–114.23)	4.03 (3.52–4.62)	6225.00 (5796.59–6653.41)	NA
	SHB	48.06 (11.40–64.78)	17.31 (0.59–53.85)	4.82 (3.72–6.25)	4450.00 (4207.30–4692.70)	NA
	TUN	226.96 (150.89–256.46)	32.65 (3.13–108.08)	8.60 (6.71–11.01)	7739.00 (6589.57–8888.43)	NA

Table 6
Continued

Source	Site/ Biome	Fungal biomass (g C m^{-2})	Bacterial biomass (g C m^{-2})	F:B ratio	SOC (g C m^{-2})	HR (g C m^{-2} yr^{-1})
	BRF	304.44 (191.19–356.01)	58.66 (7.02–171.86)	5.03 (4.23–5.98)	5812.50 (5601.96–6023.04)	NA
	TBF	88.89 (40.25–115.74)	29.88 (3.01–78.5)	4.92 (4.39–5.51)	10875.00 (9807.51–11942.49)	NA
	TCF	88.89 (40.25–115.74)	29.88 (3.01–78.5)	4.92 (4.39–5.51)	8482.50 (7974.46–8990.54)	NA
	TSF	64.42 (2.09–115.49)	51.58 (0.51–113.82)	2.22 (1.87–2.63)	8514.00 (7686.89–9341.11)	NA
	WET	70.44 (30.9–99.91)	32.96 (3.47–72.44)	4.13 (3.50–4.86)	NA	NA

[a]Simulated fungal and bacterial biomass, fungal:bacterial (F:B) ratio, soil organic carbon, and heterotrophic respiration of top 30 cm soil profile using either CLM-Microbe model or CLM4.5, values in the parentheses were 95% confidence interval. [b]Observed fungal and bacterial biomass, F:B ratio, soil organic carbon, and heterotrophic respiration from literature, values were expressed as average (range), and the values showed may not be the same as those from literature sources due to unit conversion. [c]Biome average of fungal and bacterial biomass and F:B ratio from L. L. He et al. (2020) of top 30 cm soil profile, and soil organic carbon of top 30 cm were from Jobbágy and Jackson (2000), assuming that 20–30 cm and 30–40 cm contribute equally to the soil organic carbon in 20–40 cm layer; BRF, boreal forest; DST, desert; GRS, grassland; SHB, shrub; TBF, temperate broadleaf forest; TCF, temperate coniferous forest; TSF, tropical/subtropical forest; TUN, tundra; WET, wetland. [d]Represent observed fungal and bacterial biomass, F:B ratio, soil organic carbon, and heterotrophic respiration of 0–15 cm, 0–10 cm, 5–20 cm, 0–5 cm, 0–2.3 cm and, 0–20 cm, respectively. [e]Represent observed fungal and bacterial biomass, F:B ratio, soil organic carbon, and heterotrophic respiration of 0–15 cm, 0–10 cm, 5–20 cm, 0–5 cm, 0–2.3 cm and, 0–20 cm, respectively. [f]Represent observed fungal and bacterial biomass, F:B ratio, soil organic carbon, and heterotrophic respiration of 0–15 cm, 0–10 cm, 5–20 cm, 0–5 cm, 0–2.3 cm and, 0–20 cm, respectively. [g]Represent observed fungal and bacterial biomass, F:B ratio, soil organic carbon, and heterotrophic respiration of 0–15 cm, 0–10 cm, 5–20 cm, 0–5 cm, 0–2.3 cm and, 0–20 cm, respectively. [h]Represent observed fungal and bacterial biomass, F:B ratio, soil organic carbon, and heterotrophic respiration of 0–15 cm, 0–10 cm, 5–20 cm, 0–5 cm, 0–2.3 cm and, 0–20 cm, respectively. [i]Represent observed fungal and bacterial biomass, F:B ratio, soil organic carbon, and heterotrophic respiration of 0–15 cm, 0–10 cm, 5–20 cm, 0–5 cm, 0–2.3 cm and, 0–20 cm, respectively. [j]Observed soil organic carbon of 18–60 cm. [k]Recalculated SOC from Björk et al. (2007); NA means no data available.

2.4. Model Implementation

We used default parameters for the subroutine of soil hydrological properties and methane module (Koven et al., 2013; Xu et al., 2015), and we focused on the parameterization for soil microbial mechanisms related to FBC and BBC dynamics (Table 2). To parameterize the model, we set up model simulations separately for nine sites (TSF-HS, TCF-NJ, TBF-VA, BRF-WC, SHB-OB, GRS-IA, DST-CH, TUN-MH, and WET-EM) in the phase of calibration and 12 sites (TUN-ES, TCF-NT, DST-GB, DST-JN, BRF-AL, TSF-OS, GRS-BC, TBF-SH, TBF-MS, TBF-TL, SHB-AC, and WET-EF) in the phase of validation (Table 1).

The model implementation for all sites was carried out in three stages. First, we ran the accelerated decomposition spin-up to make the system reach steady state (Thornton & Rosenbloom, 2005). Due to the differences in the length of time to reach steady state among biomes, we set the model run as 1,500 years for tropical and temperate biomes (i.e., tropical/subtropical forest, temperate coniferous forest, temperate broadleaf forest, shrub, grassland, and desert), 2,000 years for boreal and arctic biomes (i.e., boreal forest and tundra), and 3,000 years for wetlands. Then, we ran a final spin-up of 100 years to make the system ready for transient simulations during 1850–2018. Since observational FBC and BBC are reported at daily scale, we set the output resolution of transient simulations as a daily time step.

To guarantee the reasonable soil and vegetation conditions in each site at the same standard, we extracted the SOC of the top 1 m soil profile from the Harmonized World Soil Database (HWSD, https://daac.ornl.gov/cgi-bin/dsviewer.pl?ds_id=1247) and net primary productivity (NPP) from MODIS gridded data set with a spatial resolution of 30 s during 2000–2015 (http://files.ntsg.umt.edu/data/NTSG_Products/) for each site using their latitude and longitude information. Before parameterizing the CLM-Microbe model, we adjusted the parameters related to plant photosynthesis (e.g., *flnr*), C allocation (e.g., *froot_leaf*), and e-folding depth for decomposition (e.g., *decomp_depth_efolding*) to make all the sites have soil and vegetation conditions reported by global datasets. Since soil and vegetation are in high spatial heterogeneity, the global datasets may not be able to capture the variation at fine scale. If the SOC and NPP extracted from global datasets were extremely high or low for the biome, we used the values reported in the literature. If the SOC and NPP were not available from literature, we used the biome-level averages instead (Chapin

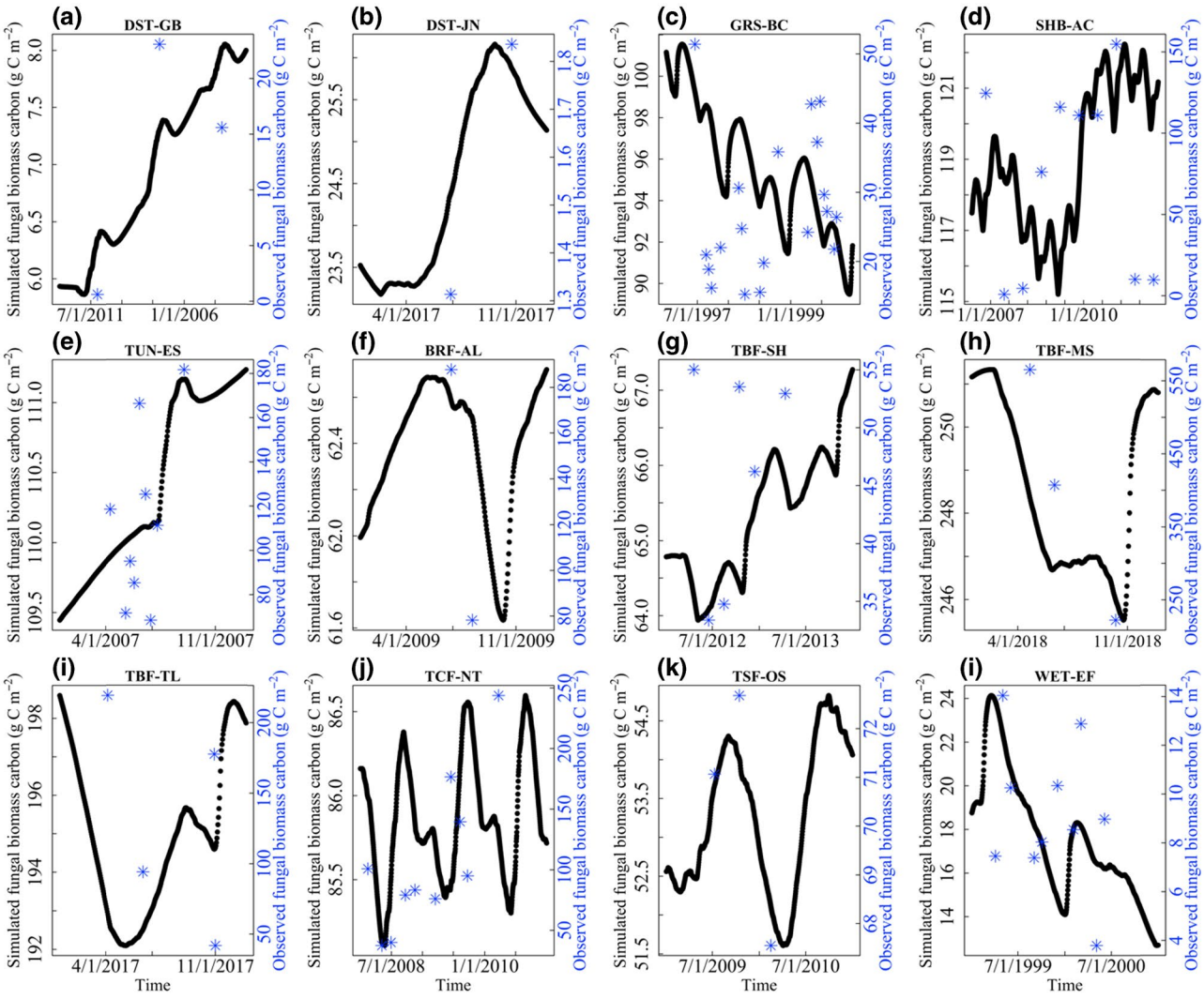

Figure 4. Model validation of fungal biomass for (a) and (b) desert, (c) grassland, (d) shrub, (e) tundra, (f) boreal forest, (g, h, and i) temperate broadleaf forest, (j) temperate coniferous forest, (k) tropical/subtropical forest, and l) wetland. The blue star indicates the observed fungal biomass, and the black filled circle represents simulated fungal biomass.

et al., 2011; Jobbágy & Jackson, 2000). For tropical/subtropical forest, we had a site specified as needleleaf trees, whereas tropical needleleaf tree is not available in default plant function types. Therefore, we modified the parameters for needleleaf_evergreen_temperate_tree following the parameters featuring tropical trees such as minimum and upper limit of temperature for growth and monthly temperature. Also, we altered the longevity for needleleaf_evergreen_temperate_tree following the trend of needle tree leaf longevity reported by Xiao (2003).

Based on the current knowledge of mechanisms for FBC and BBC dynamics, we primarily focused on parameters related to microbial lysis (*m_bdom_f*, *m_bs1_f*, *m_bs2_f*, *m_bs3_f*, *m_fdom_f*, *m_fs1_f*, *m_fs2_f*, *m_fs3_f*, *k_bacteria*, and *k_fungi*), microbial respiration (*m_batm_f* and *m_fatm_f*), decomposition of litter, DOM and SOM *(k_dom*, *m_domb_f*, *m_domf_f*, *m_doms1_f*, *m_doms2_f*, and *m_doms3_f*), and stoichiometric traits of fungal and bacterial biomass (*cn_bacteria* and *cn_fungi*). We first ran the model for each biome using the average values reported by previous studies, then we empirically calibrated the parameters based on the observed FBC and BBC of sites selected in calibration phase (Table 3). The calibration was

based on the model behavior in capturing the seasonal variations in FBC and BBC. Next, we validated the model using the parameters in Table 3 to test the model simulation performance by plotting simulated FBC and BBC against the observed data.

2.5. Model Evaluation

We used three metrics to evaluate model performance, including:

1. Mean absolute error (MAE), a measure of model error, was computed as

$$\mathrm{MAE} = \frac{1}{N}\sum_{i=1}^{N}\left|y_i - \hat{y}\right|$$

where y_i is the simulated value; $\hat{y}$ means the observed value; N is the number of data points. The MAE indicates the mean error of the model simulation, and thus lower MAE values are preferred.

2. Root mean square error (RMSE), indicating the model accuracy, was calculated as:

$$\mathrm{RMSE} = \sqrt{\frac{1}{N}\sum_{i=1}^{N}\left(y_i - \hat{y}\right)^2}$$

where y_i is the simulated value; $\hat{y}$ means the observed value; N is the number of data points. Similar with MAE, RMSE also indicates the mean error of the model simulation, and the lower values indicate the higher model accuracy. The RMSE estimation is equal or larger than MAE estimation in most cases, and the degree to which RMSE estimation exceeds MAE estimation depend on the outliers in the simulated and observed data.

3. The coefficient of determination (R^2), representing the variation in the observations explained by the model, was calculated following the equation as below,

$$R^2 = 1 - \frac{\Sigma\left(y_i - \widehat{y_i}\right)^2}{\Sigma\left(y_i - \overline{y}\right)^2}$$

where y_i is the ith simulated value; $\widehat{y_i}$ means the ith observed value; $\overline{y}$ is the mean of the observed values. Higher R^2 values indicate better performance of the model, while lower R^2 values mean the worse model performance and smaller proportion of variation being explained by the model. It is noteworthy that R^2 is not suitable for assessing the goodness-of-fit for a small number of data points due to the large bias in small samples.

2.6. Sensitivity Analysis and Uncertainty Analysis

To identify the key processes and parameters for FBC and BBC dynamics across biomes, we conducted sensitivity analysis using one site in each biome. We selected 25 parameters related to the decomposition of SOM, litter and DOM, fungal and bacterial respiration, CUE, and microbial lysis for identifying key processes and parameters in regulating FBC and BBC dynamics, which were also used for uncertainty analysis (Table 4). Eventually, nine sites, that is, DST-CH, GRS-IA, SHB-OB, TUN-MH, BRF-WC, TBF-VA, TCF-NJ, TSF-HS, WET-EM, were used for sensitivity analysis, and these sites were also used for subsequent uncertainty analysis (Figure 7, Table 5). For each parameter, we set up model simulations with +20% or −20% change in the parameter, and thus we set up 50 model simulations in total for sensitivity analysis in each site. Next, we investigated the responses of the simulated FBC, BBC, F:B ratio, SOC, and HR in surface soil (0–30 cm) during sampling period of each site. The index S, comparing the change in the model output relative to the model response for a nominal set of parameters, was calculated based on the equation following Xu et al. (2015).

$$S = \frac{\left(Ra - Rn\right) / Rn}{\left(Pa - Pn\right) / Pn}$$

where S is the ratio of the standardized change in model response to the standardized change in parameter values; R_a and R_n are model responses for altered and nominal parameters, respectively; P_a and P_n are the altered and nominal parameters, respectively. Negative S values indicate the opposite direction of model response with the regards of the direction of parameter change, and vice versa. We visualized the sensitivity analysis results using the "ComplexHeatmap" package developed by Gu et al. (2016) in R 3.5.3 for Mac OS X (R Development Core Team, 2018).

The uncertainties in FBC, BBC, F:B ratio, SOC, and HR in surface soil (0–30 cm) during the sampling period of each site were quantified using improved Latin Hypercube Sampling (LHS) approach. The LHS approach can randomly produce an ensemble of parameter combinations with high efficiency. This approach has been widely used in the modeling community to estimate uncertainties in model output (Haefner, 2005; Xu, 2010; Xu et al., 2014). First, we assumed that all parameters follow normal distribution, then we used LHS to randomly select an ensemble of 300 parameter sets using the function of "improvedLHS" in the R package "lhs" (Carnell & Carnell, 2019). Second, we computed the inverse of the standard normal cumulative distribution of 300 parameter sets using "norminv" function in MATLAB, 2018b (The MathWorks Inc., Natick, Massachusetts, USA), with the standard deviation of each parameter set as 20% of its optimal value. Third, we added the filter of setting parameters featuring fraction factors (*m_rf_s1m*, *m_rf_s2m*, *m_rf_s3m*, *m_rf_s4m*, *m_batm_f*, *m_bdom_f*, *m_bs1_f*, *m_bs2_f*, *m_bs3_f*, *m_fatm_f*, *m_fdom_f*, *m_fs1_f*, *m_fs2_f*, *m_fs3_f*, *m_domb_f*, *m_domf_f*, *m_doms1_f*, *m_doms2_f*, *m_doms3_f*) larger than 1 or smaller than 0 or the sum of an array of parameters (*m_batm_f*, *m_bdom_f*, *m_bs1_f*, *m_bs2_f*, and *m_bs3_f*, or *m_fatm_f*, *m_fdom_f*, *m_fs1_f*, *m_fs2_f*, and *m_fs3_f*, or *m_domb_f*, *m_domf_f*, *m_doms1_f*, *m_doms2_f*, and *m_doms3_f*) larger than 1 as their optimal values. Finally, we implemented the 300 model runs for each biome, and we then calculated the 95% confidence interval of FBC, BBC, F:B ratio, SOC, and SR in surface soil (0–30 cm) during experimental period of each site for reporting (Table 5).

3. Results

3.1. Model Parameterization and Validation Against Observational Data

The comparison between modeled and observed data showed that the CLM-Microbe model can capture the average and seasonal variation of FBC and BBC across biomes (Figures 2–6, Table 6). On average, the simulated FBC and BBC were consistent with the observed values, with FBC and BBC showing R^2 values of 0.70 ($P < 0.001$) and 0.26 ($P < 0.05$), respectively (Figure 6). However, FBC and BBC were underestimated by the CLM-Microbe model. For example, the simulated FBC was approximately 50% lower than the observed FBC in BRF-AL (boreal forest, BRF-) and SHB-OB (shrub, SHB-), and 40% lower than the observed FBC in DST-GB (desert, DST-) and TBF-VA and TBF-MS (temperate broadleaf forest, TBF-). Simulated BBC was 55% lower than the observed BBC in TUN-ES and TUN-MH (tundra, TUN-) and GRS-BC (grassland, GRS-), and 45% lower than the observed BBC in BRF-AL and TCF-NT (temperate coniferous forest, TCF-). The CLM-Microbe model overestimated FBC compared to the observed values in some sites; specifically, the simulated FBC was higher than the observed FBC in WET-EF and WET-EM (wetland, WET-), DST-JN, and GRS-IA. The simulated BBC was higher than the observed BBC in WET-EF, WET-EM, DST-CH, BRF-WC, SHB-AC, and TSF-HS and TSF-OS (tropical/subtropical forest, TSF-) (Figures 2–6). To compare the seasonal dynamics between observed and simulated FBC and BBC, y axes in Figures 2–5 were adjusted to facilitate the visualization of modeling results due to the systematic underestimation of FBC and BBC.

Additionally, we found relatively smaller variation (indicated as standard error, SE) in simulated FBC (SE ranging from 0.04 to 0.90 g C m^{-2}) and BBC (SE ranging from 0.02 to 0.91 g C m^{-2}) compared with the observed FBC (SE ranging from 0.26 to 99.11 g C m^{-2}) and BBC (SE ranging from 0.07 to 12.48 g C m^{-2}) (Figure 6). On average, the SE of simulated FBC and BBC was approximately 160 and 40 times smaller than the SE of observed FBC and BBC, respectively. The difference of SE in observed FBC and BBC among biomes was largely dependent on the magnitude of observed FBC and BBC (Figure 6). The highest SE of observed FBC was observed in TBF-MS (99 g C m^{-2}), BRF-AL (55 g C m^{-2}), and TUN-MH (57 g C m^{-2}). The lowest SE of observed FBC were observed in WET-EF (0.93 g C m^{-2}), WET-EM (0.26 g C m^{-2}), and DST-JN (0.26 g C m^{-2}). Compared with SE of observed FBC, SE of observed BBC was much smaller. However, SE of observed BBC were distinct among sites. We observed the highest SE of observed BBC in TUN-MH (12 g C m^{-2}), and

TBF-MS (12 g C m^{-2}). The SE of observed BBC was lowest in TBF-SH (0.40 g C m^{-2}), WET-EF (0.24 g C m^{-2}), TSF-HS (0.18 g C m^{-2}), and WET-EM (0.07 g C m^{-2}).

Due to the large difference in variations of simulated and observed FBC and BBC, we estimated the simulated FBC and BBC dynamics using relative change in FBC and BBC, that is, the difference between individual and the average of biomass over the average of biomass during the study period (Table 4). In the calibration phase, MAE ranged from 0.06 to 1.16 for FBC and from 0.06 to 1.04 for BBC, while RMSE ranged from 0.07 to 1.43 for FBC and from 0.07 to 1.11 for BBC. In the validation phase, MAE ranged from 0.01 to 0.73 for FBC and from 0.04 to 1.18 for BBC, while RMSE ranged from 0.02 to 0.79 for FBC and from 0.04 to 2.02 for BBC. Although the model explained the FBC and BBC dynamics well in most sites, particularly TBF-MS ($R^2 = 0.94$ for FBC and $R^2 = 0.95$ for BBC) and TSF-OS ($R^2 = 0.98$ for FBC and $R^2 = 0.52$ for BBC), the simulation in some sites for FBC (GRS-IA, SHB-OB, GRS-BC, SHB-AC, TBF-TL, TBF-SH, TCF-NT, and WET-EF) and BBC (TSF-HS, GRS-BC, TUN-ES, and WET-EF) was relatively poor, with R^2 smaller than 0.1. It is noteworthy that the number of data points ranges from 2 to 13 for FBC and BBC data across sites, which is much smaller than 30, the threshold for a large sample. The R^2 may not be suitable for assessing the goodness-of-fit for a small number of data points due to the large bias in small samples, although it is widely used in model performance estimation. For example, R^2 was 0.005 for FBC and 0.299 for BBC in SHB-OB, while MAE (0.06 for FBC and BBC) and RMSE (0.07 for FBC and BBC) were small, indicating small biases in the simulated FBC and BBC.

3.2. Sensitivity Analysis

We found high sensitivity of FBC and BBC dynamics to parameters that related to microbial turnover and C:N ratio of fungal and bacterial biomass across biomes (Figure 7). Fungal biomass turnover rate (*k_fungi*) had negative effects on FBC and F:B ratio across biomes, while bacterial biomass turnover rate (*k_bacteria*) had negative and positive effects on BBC and F:B ratio, respectively. The C:N ratio of bacterial biomass (*cn_bacteria*) had negative, positive, and negative effects on FBC, BBC, and F:B ratio, respectively. In contrast, C:N ratio of fungal biomass (*cn_fungi*) had positive, negative, and positive effects on FBC, BBC, and F:B ratio, respectively. A 20% increase or decrease in *k_fungi* and *k_bacteria* led to different magnitudes of negative effects on FBC and BBC, respectively, across biomes. While a 20% decrease in *k_fungi* and *k_bacteria* led to the S values around -1.25 and -1.30 for FBC and BBC, a 20% increase in *k_fungi* and *k_bacteria* resulted in S values around -0.85 and -0.84 for FBC and BBC, respectively. Changes in *k_bacteria* had similar magnitudes of positive effects on F:B ratio, with S values around 1.00 for both 20% increase and decrease in *k_bacteria*. While a 20% increase or decrease in *k_fungi* had different magnitudes of negative effects on F:B ratio, with a 20% decrease or increase in *k_fungi* leading to S values around −1.27 and −0.85, respectively, across biomes. The higher S values suggested that FBC and BBC were more sensitive to decreases in *k_fungi* and *k_bacteria*, which would induce larger increases in FBC and BBC; in particular, a 20% decrease in *k_fungi* led to higher sensitivity of F:B ratio.

In addition, FBC and BBC were closely correlated with the decomposition of SOM and DOM and microbial respiration (Figure 7). Fraction factors quantifying C flow from SOM to soil microbes (*m_rf_s1m*, *m_rf_s2m*, *m_rf_s3m*, and *m_rf_s4m*) were positively correlated with FBC and BBC. However, the magnitude of the *m_rf_s4m* on FBC and BBC were different among biomes. The highest response was in TSF-HS (S = 1.03 for FBC and S = 1.08 for BBC with -20% change vs. S = 1.42 for FBC and S = 1.49 for BBC with +20% change), while the lowest response was in BRF-WC (S = 0.28 for FBC and S = 0.26 for BBC with −20% change vs. S = 0.28 for FBC and S = 0.24 for BBC with +20% change). In addition, we found a positive correlation between the fraction factor quantifying C flow from DOM to fungal biomass (*m_domf_f*) and FBC and F:B ratio and a positive correlation between fraction factor quantifying C flow from DOM to bacterial biomass (*m_domb_f*) and BBC, and a negative correlation between *m_domb_f* and F:B ratio. However, the magnitudes varied among biomes, with FBC being most sensitive to *m_domf_f* in GRS-IA (S = 0.432), BBC being most sensitive to *m_domb_f* in TBF-VA (S = 0.593), and F:B ratio being most sensitive to *m_domf_f* in GRS-IA (S = 0.415) and *m_domb_f* in TBF-VA (S = −0.630) with -20% change. In contrast, FBC, BBC, and F:B ratio were insensitive to *m_domb_f* and *m_domf_f* in BRF-WC, with the absolute S values close to 0.001. Moreover, we found weak positive effects of fraction factors quantifying C flow from DOM to SOM (*m_doms1_f*, *m_doms2_f*, and *m_doms3_f*) on FBC and BBC across biomes. Across biomes, FBC, BBC,

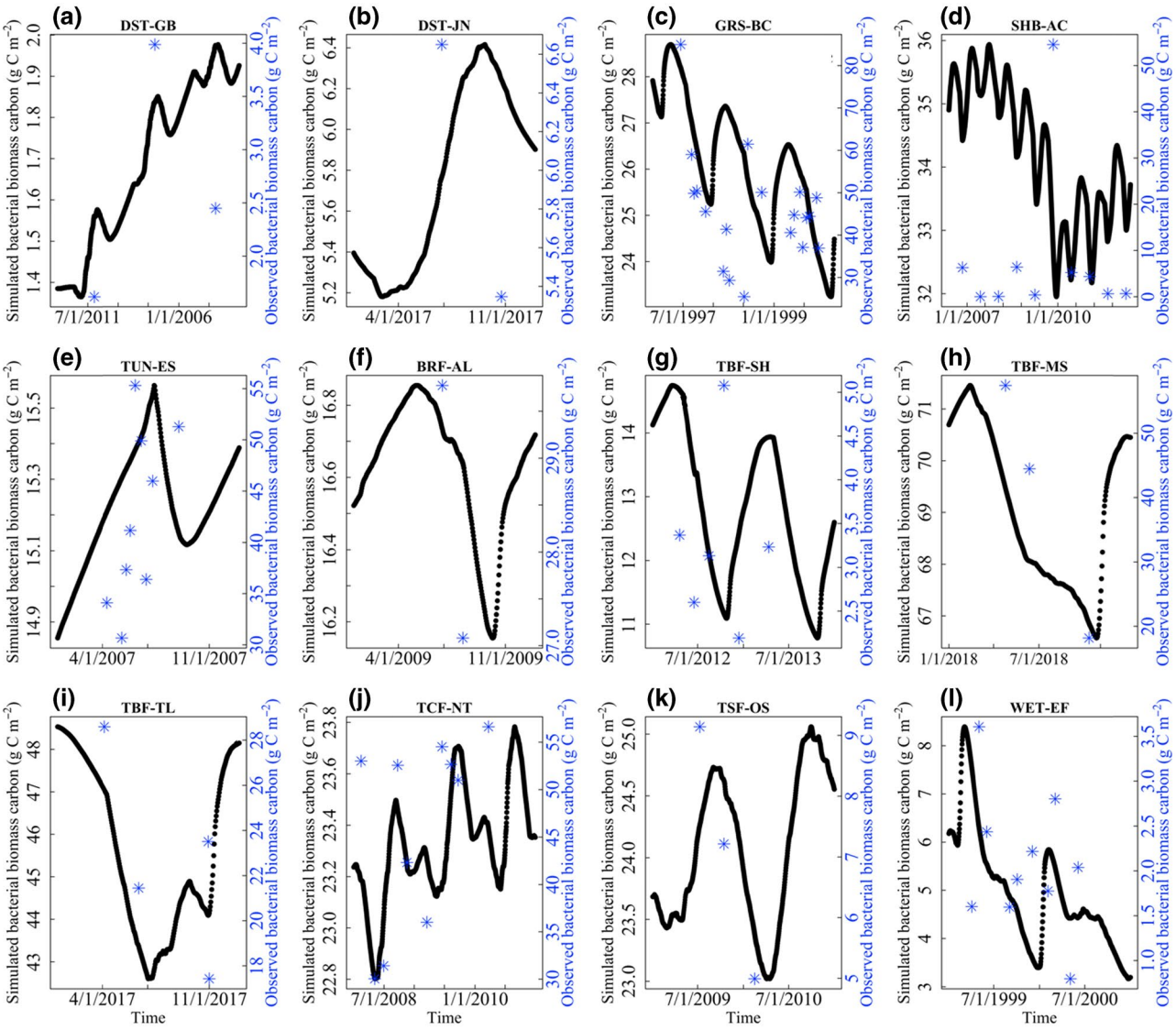

Figure 5. Model alidation of bacterial biomass for (a) and (b) desert, (c) grassland, (d) shrub, (e) tundra, (f) boreal forest, (g, h, and i) temperate broadleaf forest, (j) temperate coniferous forest, (k) tropical/subtropical forest, and l) wetland. The blue star indicates the observed bacterial biomass, and the black filled circle represents simulated bacterial biomass.

F:B ratio, SOC, and HR in surface soil (0–30 cm) were insensitive to maximum microbial CUE (CUE_{max}). We observed a higher negative correlation between fraction factor quantifying C being respired by fungi (*m_fatm_f*) and FBC and between the fraction factor quantifying C being respired by bacteria (*m_batm_f*) and BBC in GRS-IA, TSF-SH, and TCF-NJ, with S values ranging from −0.104 to −0.044 of *m_fatm_f* for FBC and from −0.615 to −0.023 of *m_batm_f* for BBC, while FBC and BBC in other biomes were insensitive to *m_batm_f* and *m_fatm_f* change.

The SOC was positively correlated with fraction factors quantifying C flow from SOM to soil microbes (*m_rf_s1m*, *m_rf_s2m*, *m_rf_s3m*, or *m_rf_s4m*), while SOC was negatively correlated with fraction factor quantifying C being respired by bacteria (*m_batm_f*) and fungi (*m_fatm_f*), but the magnitudes varied among biomes (Figure 7). We found highly positive correlations between *m_rf_s1m*, *m_rf_s2m*, *m_rf_s3m*, or *m_rf_s4m* and SOC across biomes except for tundra and boreal forest. The parameters of *m_batm_f* and *m_fatm_f* were negatively correlated with SOC, but the magnitudes varied among biomes. Specifically, we found higher negative correlation between *m_batm_f* and SOC in TBF-VA (S = −0.10 with −20% and

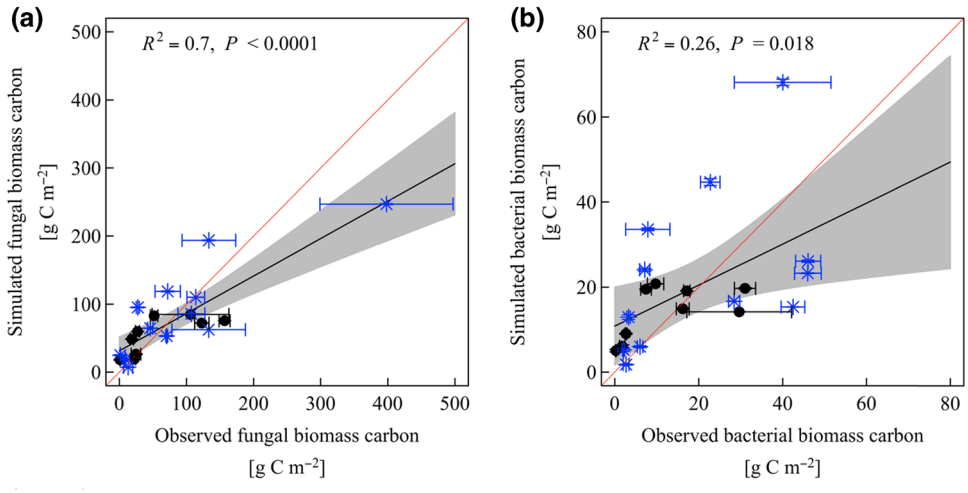

Figure 6. Comparison of the averaged observed and simulated (a) fungal and (b) bacterial biomass. The blue star indicates the (a) fungal or (b) bacterial biomass in calibration phase, and the black filled circle represents (a) fungal or (b) bacterial biomass in validation phase; vertical and horizontal error bars indicate standard error of simulated and observed values, respectively, for both (a) fungal and (b) bacterial biomass.

+20% change), TCF-NJ (S = −0.08 with -20% and +20% change), and TSF-HS (S = −0.10 with −20% and +20% change). While *m_fatm_f* was more negatively correlated with SOC in GRS-IA (S = −0.12 with −20% and +20% change), TCF-NJ (S = −0.10 with −20% and +20% change), and TSF-HS (S = −0.17 with −20% and +20% change). The SOC in other biomes were relatively insensitive to changes in *m_batm_f* (S values ranging from −0.06 to −0.02) and *m_fatm_f* (S values ranging from −0.05 to −0.03). Across biomes, we only found strong negative correlations between *m_doms1_f*, *m_doms2_f*, and *m_doms3_f* and SOC in TCF-NJ (S = −0.08 for *m_doms1*, S = −0.12 for *m_doms2*, and S = −0.18 for *m_doms3*).

HR widely responded of to all parameters listed for soil microbial mechanisms, but in low sensitivity (Figure 7). Specifically, the HR in sites such as DST-CH, GRS-IA, TBF-VA, TCF-NJ, and TSF-HS showed a weak response to changes in all parameters. However, we also found relatively stronger negative correlations between *m_batm_f* and HR in BRF-WC (S = −0.09 with −20% change and S = −0.12 with +20% change) and WET-EM (S = −0.08 with −20% change and S = −0.11 with +20% change).

3.3. Simulated FBC, BBC, F:B Ratio, SOC, and HR at Annual Scale

Annual estimation of FBC, BBC, F:B ratio, SOC, and HR in the top 30 cm soils derived from the CLM-Microbe model showed large variations among biomes (Table 5). The simulated FBC was the highest in TCF-NJ (380 g C m^{-2}), followed by TBF-VA (259 g C m^{-2}), BRF-WC (205 g C m^{-2}), and TUN-MH (180 g C m^{-2}), while it was lowest in WET-EM (24 g C m^{-2}) with a range of 14–40 g C m^{-2}. The simulated FBC in the top 30 cm of soils in DST-CH, GRS-IA, SHB-OB, TUN-MH, BRF-WC, TBF-VA, TCF-NJ, TSF-HS, and WET-EM was 1.6 (0–15 cm), 5.9 (0–10 cm), 0.9 (0–10 cm), 1.7 (0–10 cm), 4.0 (5–20 cm), 2.1 (0–5 cm), 14.0 (0–2.3 cm), 1.7 (0–10 cm), and 22.6 (0–20 cm) times of the observed FBC (at varying soil depths), respectively. Compared with the global data set of FBC and BBC (L. He et al., 2020), the simulated FBC in the top 30 cm of soils was generally consistent with the biome-averaged FBC in the top 30 cm of the soils. The model simulated FBC in DST-CH, GRS-IA, TUN-MH, BRF-WC, and TSF-HS was similar with the biome-averaged FBC in the top 30 cm of soils. However, we detected extreme FBC simulated by the model in some sites compared with the biome-averaged FBC. The CLM-Microbe model simulated higher FBC in SHB-OB, TBF-VA and TCF-NJ and lower FBC in WET-EM relative to their corresponding the biome-averaged FBC in the top 30 cm soils.

The simulated BBC was the highest in TCF-NJ (100 g C m^{-2}), followed by TBF-VA (70 g C m^{-2}), BRF-WC (40 g C m^{-2}), and TUN-MH (30 g C m^{-2}), while the simulated BBC was the lowest in WET-EM (7 g C m^{-2}) and DST-CH (9 g C m^{-2}). The simulated BBC in the top 30 cm of soils in DST-CH, GRS-IA, SHB-OB, TUN-

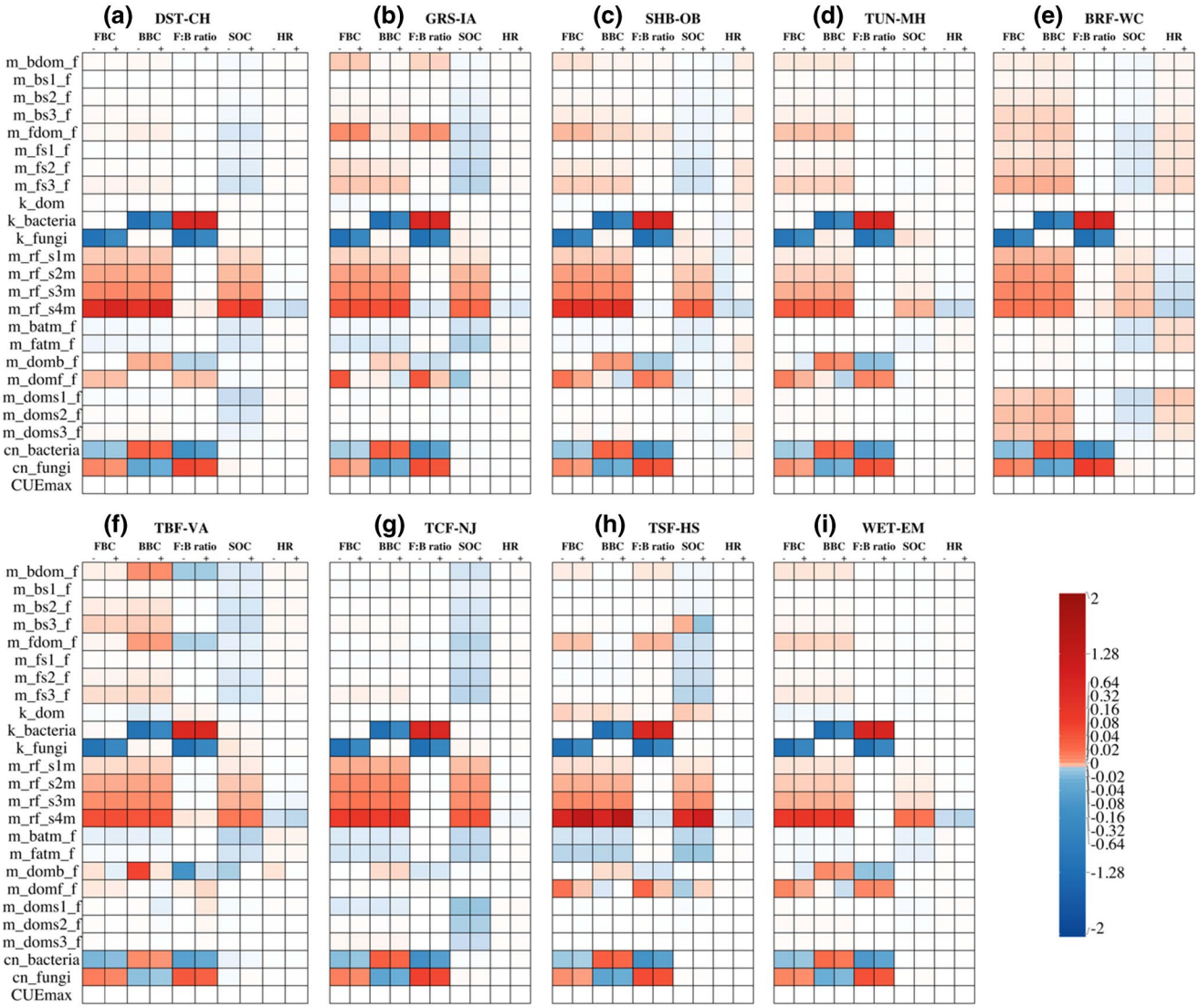

Figure 7. Sensitivity analysis for model response of fungal biomass, bacterial biomass, F:B ratio, soil organic carbon, and soil microbial respiration in the top 30 cm to 25 parameters (m_bdom_f, m_bs1_f, m_bs2_f, m_bs3_f, m_fdom_f, m_fs1_f, m_fs2_f, m_fs3_f, k_dom, k_bacteria, k_fungi, m_rf_s1m, m_rf_s2m, m_rf_s3m, m_rf_s4m, m_batm_f, m_fatm_f, m_domb_f, m_domf_f, m_doms1_f, m_doms2_f, m_doms3_f, cn_bacteria, cn_fungi, and CUEmax) in (a) desert, (b) grassland, (c) shrub, (d) tundra, (e) boreal forest, (f) temperate broadleaf forest, (g) temperate coniferous forest, (h) tropical/subtropical forest, and (i) wetland. "+" and "-" indicate 20% increase or 20% decrease of parameter values. CUE, carbon use efficiency; FBC, fungal biomass carbon; BBC, bacterial biomass carbon; F:B ratio, fungal:bacterial biomass carbon ratio; SOC, soil organic carbon; HR, heterotrophic respiration; Dark red and darker blue indicate a stronger positive or negative model response of the variable to parameter change. S is negative if the direction of model response opposes the direction of parameter change during the sampling years for all sites.

MH, BRF-WC, TBF-VA, TCF-NJ, TSF-HS, and WET-EM was 5.0 (0–15 cm), 2.1 (0–10 cm), 2.2 (0–10 cm), 1.0 (0–10 cm), 4.1 (5–20 cm), 2.3 (0–5 cm), 13.5 (0–2.3 cm), 6.3 (0–10 cm), and 25.4 (0–20 cm) times of the observed BBC (at varying soil depths), respectively. Compared with the global data set of FBC and BBC (L. He et al., 2020), the simulated BBC in DST-CH, GRS-IA, TUN-MH, and BRF-WC was similar with their corresponding biome-averaged BBC in the top 30 cm soils. However, the simulated BBC was higher in SHB-OB, TBF-VA, and TCF-NJ and lower in TSF-HS and WET-relative to their corresponding biome-averaged BBC in the top 30 cm soils.

The simulated F:B ratio was the highest in TUN-MH (6.30), followed by BRF-WC (5.39), DST-CT (4.54), SHB-OB (4.16), and TCF-NJ (3.96), the F:B ratio was the lowest in TSF-HS (2.31). The observed F:B ratio was highly variable, with the highest F:B ratio in DST-CH (14.1, 0–15 cm), followed by SHB-OB (9.1, 0–10 cm)

and BRF-WC (5.3, 5–20 cm), while GRS-IA (1.1, 0–10 cm) featured the lowest F:B ratio among biomes. Compared with our recently compiled global data set of FBC and BBC (L. He et al., 2020), the CLM-Microbe model simulated F:B ratio was generally consistent with the biome-averaged F:B ratio in the top 30 cm soils. Similar as the CLM-Microbe model simulated F:B ratio, the highest biome-averaged F:B ratio was found in tundra (8.6), followed by boreal forests (5.0), temperate forests (4.9), and shrub (4.8), while the lowest biome-averaged F:B ratio was found in tropical/subtropical forests (2.2).

Large variations were found in the simulated SOC of top 30 cm among biomes, with SOC highest in WET-EM (13,204 g C m^{-2}), which was 5.3 times of that in the site with the lowest values, that is, TSF-HS (2,509 g C m^{-2}). BRF-WC (8,685 g C m^{-2}) has the second largest SOC, followed by TCF-NJ (7,990 g C m^{-2}), TBF-VA (5,873 g C m^{-2}), and TUN-MH (3,604 g C m^{-2}) (Table 5). Similar as the CLM-Microbe model, CLM4.5 simulated-SOC in top 30 cm was high in WET-EM (9,951 g C m^{-2}) and low in SHB-OB (1,598 g C m^{-2}) and TUN-MH (2086 g C m^{-2}). In contrast, CLM4.5 simulated-SOC in top 30 cm was much higher in GRS-IA (11,991 g C m^{-2}), TBF-VA (11,239 g C m^{-2}), and TSF-HS (6,628 g C m^{-2}) compared with that simulated by the CLM-Microbe model. It is worthwhile to note that DST-CH (0 g C m^{-2}) featured the lowest SOC in the top 30 cm simulated by CLM4.5 among sites owing to the vegetation mortality. The simulated SOC in the top 30 cm was slightly lower than the average derived from a global data set of SOC (Jobbágy & Jackson, 2000). However, the simulated SOC in BRF-WC was slightly higher than that of biome-averaged SOC in the top 30 cm. Excluding wetlands due to lack of available data, the biome-averaged SOC is consistent with the simulated SOC in the top 30 cm. The SOC is higher in temperate broadleaf forest (10,875 g C m^{-2}), temperate coniferous forest (8,483 g C m^{-2}), and tundra (7,739 g C m^{-2}). In contrast to the lowest simulated SOC in the top 30 cm in TSF-HS (2,509 g C m^{-2}), the biome-averaged SOC in the top 30 cm was lowest in the desert (2,728 g C m^{-2}).

The fraction of SOC in microbial biomass (FBC and BBC combined) showed a large variation among biomes, with the proportion ranging from 0.2% to 6.0% (Table 5). The proportion was the highest in TCF-NJ (6.0%), followed by TUN-MH (5.80%), TBF-VA (5.60%), SHB-OB (5.50%), and GRS-IA (5.40%), WET-EM (0.23%) featured the lowest proportion between the sum of FBC and BBC and SOC among biomes. Similarly, the biome-averaged proportion between the sum of FBC and BBC and SOC ranged from 1.1% to 6.2% among biomes. However, the rank of the biome-averaged proportion between the sum of FBC and BBC and SOC was different with that simulated by the CLM-Microbe model. The proportion between the sum of FBC and BBC and SOC was highest in boreal forests (6.2%) and lowest in temperate broadleaf forests (1.1%). Tundra had the second highest proportion between the sum of FBC and BBC and SOC (3.4%), followed by desert (2.7%), grassland (2.2%), shrub (1.5%), and then tropical/subtropical forest and temperate coniferous forest (1.4%).

The CLM-Microbe model simulated annual estimation of HR was the highest in TCF-NJ (811 g C m^{-2} yr^{-1}), which was about nine times of that in the lowest site, that is, TUN-MH (93 g C m^{-2} yr^{-1}) (Table 5). We found second highest HR in TBF-VA (560 g C m^{-2} yr^{-1}), followed by WET-EM (540 g C m^{-2} yr^{-1}), BRF-WC (420 g C m^{-2} yr^{-1}), and TSF-HS (401 g C m^{-2} yr^{-1}). Compared with the CLM-Microbe model, CLM4.5 simulated highly consistent HR in TBF-VA, WET-EM, TSF-HS, SHB-OB, and TUN-MH. However, we observed much higher HR in GRS-IA simulated by CLM4.5 (757 g C m^{-2} yr^{-1}), which was 2.4 times of that simulated by the CLM-Microbe model (313 g C m^{-2} yr^{-1}).

3.4. Simulated Time-Series C Flow into and out of FBC and BBC

The dynamics and magnitude of C flow related to the decomposition of litter, SOM, and DOM, HR, and microbial lysis for FBC and BBC differed among biomes, while the seasonal patterns of those C flows were similar for fungi and bacteria in each biome (Figures 8 and 9). In the CLM-Microbe model, FBC and BBC assimilate C from the decomposition of litter, SOM, and DOM, the dominance of these C flows varied temporally and among biomes. The C flow from litter decomposition predominated fungal and bacterial C assimilation year-round at a few sites such as DST-CH (Figures 8a and 9a), TUN-MH (Figures 8i and 9i), and TSF-HS (Figures 8h and 9h). We also found the dominant role of litter decomposition on fungi and bacteria C assimilation in GRS-IA (Figures 8b and 9b), TBF-VA (Figures 8f and 9f), and WET-EM during the nongrowing seasons (Figures 8i and 9i). The fungal and bacterial C assimilation at sites such as BRF-WC (Figures 8e and

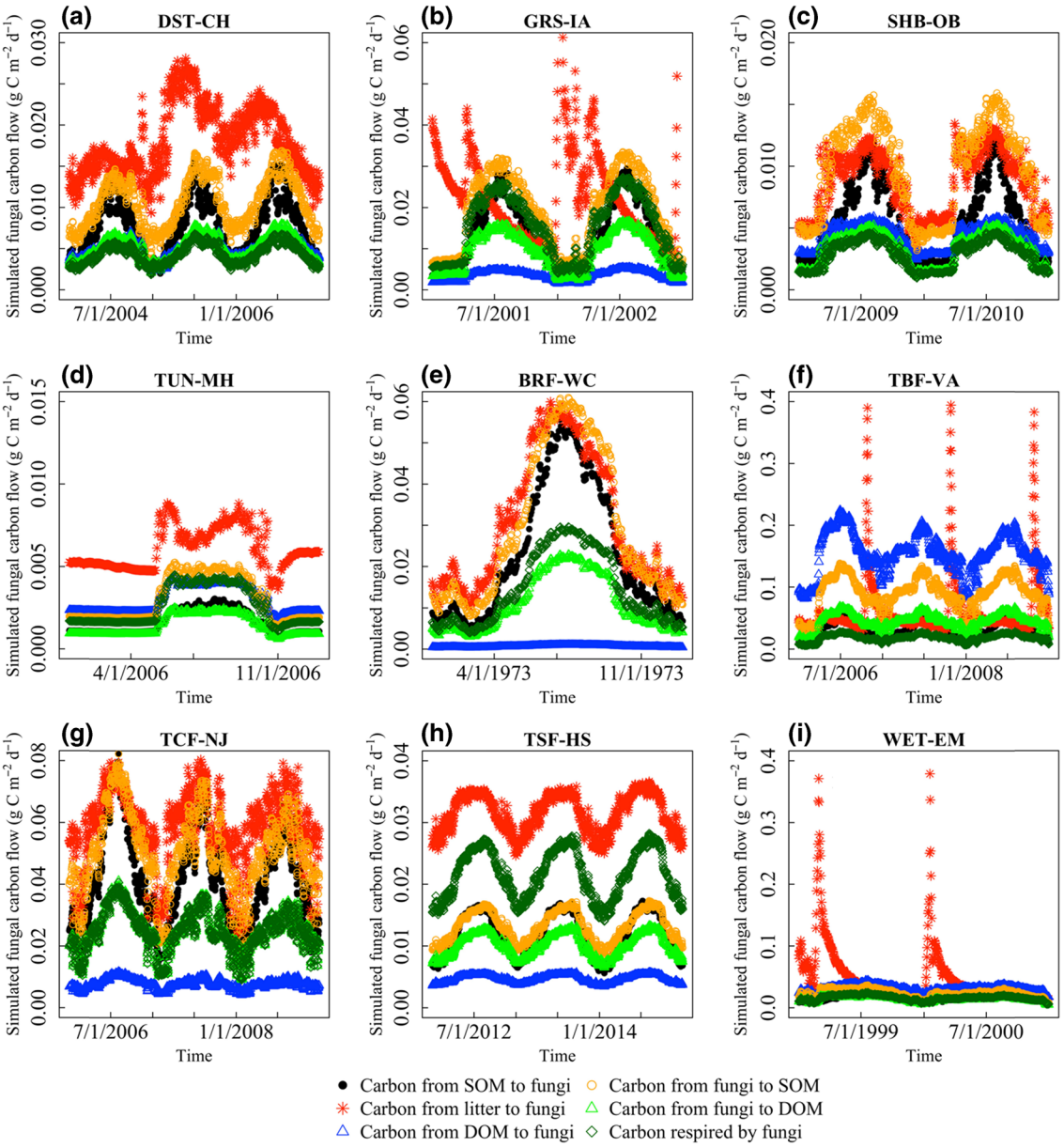

Figure 8. Time-series of simulated carbon flow into and out of the bacterial biomass carbon pool.

9e), SHB-OB (Figures 8c and 9c), and TCF-NJ (Figures 8g and 9g) were co-dominated by the decomposition of litter and SOM. The decomposition of DOM is the least important pathway for fungal and bacterial C gain across biomes; however, we observed the predominant role of the DOM decomposition on fungal and bacterial C assimilation at TBF-VA (Figures 8f and 9f) and WET-EM (Figures 8i and 9i) during the whole year, and second largest C assimilation of DOM decomposition at TUN-MH (Figures 8d and 9d), and temporarily dominant role of DOM decomposition during winter and spring at SHB-OB (Figures 8c and 9c).

The C loss from fungal and bacterial biomass was primarily represented as microbial respiration and microbial lysis in the CLM-Microbe model. The C flow from fungal and bacterial biomass to SOM during microbial lysis was the predominant mechanism of C loss at DST-CH (Figures 8a and 9a), SHB-OB (Figures 8c and 9c), BRF-WC (Figures 8e and 9e), TBF-VA (Figures 8f and 9f), and TCF-NJ (Figures 8g and 9g). However, we also observed the co-dominance of C flow from fungal and bacterial biomass to SOM and microbial respiration in controlling fungal and bacterial C loss at GRS-IA (Figures 8b and 9b), and TUN-MH (Figures 8d

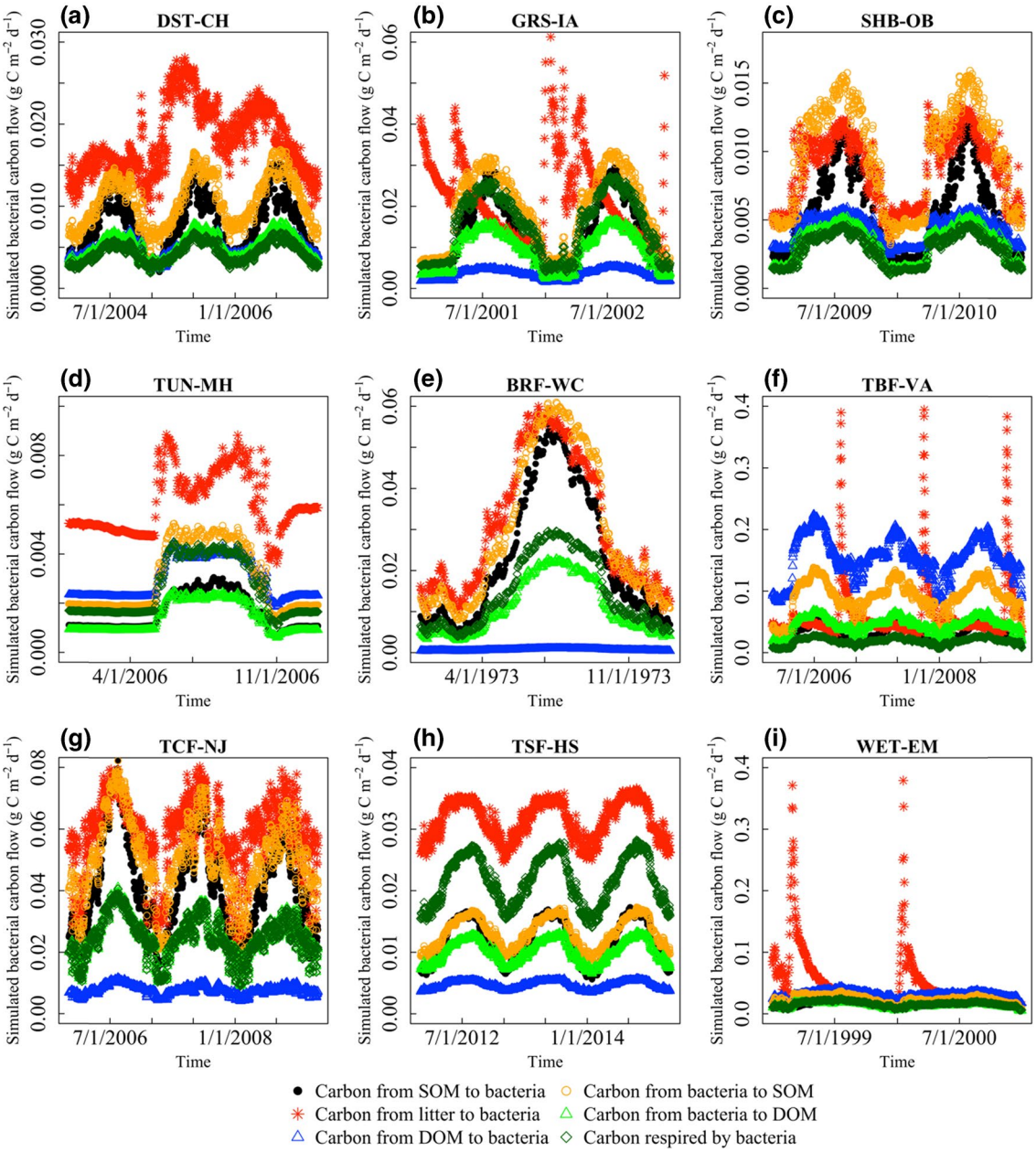

Figure 9. Time-series of simulated carbon flow into and out of the bacterial biomass carbon pool.

and 9d). The fungal and bacterial C loss were co-determined by C flow from fungal and bacterial biomass to SOM and DOM and microbial respiration at WET-EM (Figures 8i and 9i). While we found the predominant role of microbial respiration in regulating fungal and bacterial C loss in TSF-HS, microbial lysis contributed less to fungal and bacterial C loss (Figures 8h and 9h).

4. Discussion

4.1. Model Performance and Comparison with Existing Models

The CLM-Microbe model simulated FBC and BBC are consistent with the observed FBC and BBC, with a slight underestimation (Figures 2–6; Table 6). Similar as our study, G. Wang et al. (2015) reported that the

MEND model can adequately capture the soil microbial biomass C dynamics with the representation of soil microbial processes such as microbial dormancy, microbial enzyme production, and enzyme catalyzing effects on decomposition. The TRIPLEX-MICROBE model can also estimate the global- and biome-level soil microbial biomass C with reasonable accuracy (K. Wang et al., 2017). Meanwhile, studies found that soil microbial traits play a key role in soil microbial biomass accumulation. G. Wang et al. (2015) compared the simulated soil microbial biomass C by MEND with and without dormancy, and they found that MEND model without dormancy largely underestimated the soil microbial biomass C. In the CLM-Microbe model, the soil microbial community, represented by active fungi and bacteria, is directly related to many biogeochemical processes such as decompositions of litter, DOM, and SOM. The accumulations of FBC and BBC could largely affect soil respiration and soil C pools such as SOM. To ensure reasonable soil conditions, we finalized the parameters related to soil microbial processes by ensuring consistency between simulated SOC with the SOC reported in global datasets. Therefore, the missing representation of dormancy may be responsible for the slight underestimation of FBC and BBC in the CLM-Microbe model.

Additionally, the CLM-Microbe model simulated FBC and BBC showed smaller variation compared with the observed FBC and BBC, respectively (Figure 6). Soil microbial communities are not static, with microbial biomass showing temporal dynamics (Björk et al., 2008; Lipson et al., 2002; Lipson & Schmidt, 2004). This variation is highly associated with environmental factors such as soil temperature and soil moisture (Devi & Yadava, 2006). Meanwhile, plant-produced C also control soil microbial growth, as confirmed by studies that reported positive correlation between soil microbial biomass and aboveground litter input (Feng et al., 2009) and root exudates (Göttlicher et al., 2006). Although we incorporated the vegetation effects in soil microbial biomass in the form of DOM released into soil, the decomposition of DOM will promote C availability for soil microbes, the stimulating effects of DOM on microbial activity was not included in the present CLM-Microbe model. In addition, soil food web was not explicitly incorporated into the CLM-Microbe model, even the turnover rate of soil microbial biomass was probably regulated by their predators such as nematodes, mites, and protozoa (CPD et al., 1995; Ingham et al., 1986). The predator activity can induce abrupt changes in soil microbial biomass; for example, Buckeridge et al. (2013) observed seasonal variation in soil microbial community structure, and the decline in FBC from winter to late winter, and then again in spring, was closely associated with the high abundance of protozoa. Furthermore, only a small proportion of the soil microbial community is active, while the majority is dormant, that is, a reversible state of low to zero metabolic activity (Cole, 1999). Soil microbes can determine whether the environmental conditions are suitable for microbes to remain viable within short time periods (Garcia-Pichel & Pringault, 2001). Therefore, the rapid change in soil microbial state can lead to abrupt changes in soil microbial biomass (Y. He et al., 2015). However, in the CLM-Microbe model, we assumed that the activity of fungi and bacteria are regulated by soil environmental conditions such as soil temperature, soil moisture, and soil oxygen concentration (Section 2.2).

4.2. Controls on Soil Microbial Community Composition

Turnover rates of FBC and BBC are the most important factors regulating FBC and BBC dynamics across biomes, respectively, with increasing turnover rate of fungi decreased FBC and F:B ratio, and increasing turnover rate of bacteria decreased BBC and increased F:B ratio (Figure 7). Turnover rate, the inverse of lifespan, can be mathematically calculated by dividing the production by the biomass pool size. In the microbial world, biomass turnover is much faster relative to that of plants and animals in natural environments, microbial related biogeochemical fluxes are closely linked to turnover and succession of microbial communities (Schmidt et al., 2007). Higher estimates for biomass production consequently correspond to lower turnover times, and vice versa (Pritchard et al., 2008; Rousk & Bååth, 2007). Therefore, the increase in turnover rate of fungi and bacteria is expected to induce declining FBC and BBC, respectively. The increasing turnover rate of fungi will decrease the dominance of fungi, and thus narrowed F:B ratio. In contrast, the increasing bacterial turnover rate would suppress the bacterial dominance and thus a broadening F:B ratio.

In addition, we observed the important role of fungal and bacterial biomass C:N ratio in regulating FBC, BBC, and F:B ratio, with rising fungal biomass C:N ratio increased FBC and F:B ratio and rising bacterial

biomass C:N ratio increased BBC and decreased F:B ratio (Figure 7). The C cycle is closely coupled with that of other essential elements, and the proportion of substrate C being respired by soil microbes is closely related to substrate C:N ratio, with more C being respired when substrate has high C:N ratio or low N concentration (Spohn, 2015). In addition, the ratio between the substrate and the microbial biomass C:N ratio determines the proportion of C being assimilated by soil microbes (Sinsabaugh et al., 2013), which was directly reflected as CUE and adopted into the CLM-Microbe model. Fungi and bacteria have distinct C and nutrient compositions, with C:N ratio averaged around 5 for bacteria and 12 for fungi (Strickland & Rousk, 2010), their C:N ratios specifically determine the partitioning coefficient of C between fungi and bacteria in the CLM-Microbe model. Increasing fungal biomass C:N ratio will thus increase the proportion of C assimilated by fungi and promote the dominance of fungi, while increasing bacterial biomass C:N ratio stimulates the C flow toward bacteria and suppresses the fungal C gain, and thereby decreasing F:B ratio.

The FBC, BBC, and F:B ratio were also positively affected by the C flow from SOM to soil microbes. We observed higher sensitivity of FBC and BBC in desert and tropical/subtropical sites to changes in C flow from SOM to soil microbes (Figure 7). The increase in microbial C gain from SOM will enhance the C and energy availability for soil microbial growth, which is thus reflected as an increase in soil microbial biomass. In the model, fungal and bacterial C gain from SOM is first expressed as the C input from SOM to soil microbes as a whole, then the C was partitioned by FBC and BBC pools based on the C:N ratio of their biomass, the biomass pool with higher C:N ratio is expected to gain higher proportion of C (Figure 1; Section 2.2). In other words, the C flow from SOM to soil microbes will determine the overall received C from SOM for both fungi and bacteria. Although there are large variations in fungal (3–60) and bacterial (3–12) biomass C:N ratio, indicating that a large proportion of fungi and bacteria overlap with regards to biomass C:N ratio, fungi tend to have higher mean C:N ratio (Strickland & Rousk, 2010). Accordingly, we assigned higher C:N ratio for fungal (*cn_fungi*) relative to bacterial (*cn_bacteria*) biomass, and the reasonability of these parameters were validated and tested by observed FBC and BBC dynamics (Table 3). As a result, the increase in microbial C gain from SOM will enhance FBC and BBC; however, FBC increase will be promoted more due to its higher C:N ratio, thereby exhibiting an increase in F:B ratio.

The FBC, BBC, and F:B ratio in DST-CH and TSF-SH showed relatively higher sensitivity to soil microbial C assimilation from SOM decomposition, which is likely result from the favorable soil moisture and temperature for decomposition. Tropical and subtropical forests are known to have higher decomposition rate due to the high annual precipitation and temperature, while decomposition in deserts is widely reported to be limited by soil moisture (Chapin et al., 2011). Despite the general recognition of water limitation in deserts, the desert site (DST-CH) in this study has a mean annual precipitation of 380 mm, which is pretty high compared to "common" deserts (Bell et al., 2014). Given the high sensitivity of SOM decomposition to soil moisture condition, the higher water availability may enhance SOM decomposition in TSF-SH and DST-CH (Chapin et al., 2011). Furthermore, DST-CH is vegetated by herbaceous plant species, the higher proportion of nonwoody components will improve the decomposability of substrates (Koven et al., 2013). In addition, although water limitation decreases the activity of soil microbes, primarily bacteria, fungi are more tolerant to drought due to their hyphal water uptake capability and dominate SOM decomposition in dry environmental conditions such as deserts (Yuste et al., 2011). Therefore, the decomposition of SOM plays an important role for fungal and bacterial C turnover, and fungal growth tends to be promoted more due to higher biomass C:N ratio and tolerance to water stress, leading to an increase in F:B ratio.

4.3. Controls on Soil Organic C Density and HR

The C flow from SOM to soil microbes enhanced SOC, but this enhancement is weak in tundra and boreal forest; soil microbial respiration strongly decreased SOC in forests except for boreal forest (Figure 7). In addition to processing SOM from other organic C forms, soil microbes contribute to the formation of persistent SOM via necromass (Gougoulias et al., 2014). Soil microbial necromass is about three orders of magnitude higher than soil microbial biomass (Glaser et al., 2004), and can make up more than half of SOC (Liang et al., 2019). Soil microbial necromass is directly related to soil microbial biomass turnover rate, the slow biomass turnover rate in boreal forests and tundra might be one of the important reasons for low SOC sensitivity to soil microbial biomass C gain from SOM (Table 3). Moreover, boreal forests and tundra are

known to have low soil temperature, indicating smaller temperature effects on soil microbial community lysis. As a result, low biomass turnover rate of fungi and bacteria as well as low soil temperature may lead to the long persistence of organic C in soil microbial biomass, resulting in the lower contribution of soil microbial necromass to SOM. Compared with boreal forests, soil moisture and soil temperature in temperate and tropical forests are relatively desirable for soil microbial activity, and thus the decomposition process is more favorable in temperate and tropical forests. Higher decomposition in temperate and tropical forests is indicated by the C released as CO_2 by fungi and bacteria in the CLM-Microbe model (Table 5). Therefore, in temperate and tropical forests, the higher proportion of C respired by fungi and bacteria will more prominently decrease C remaining in the ecosystem, leading to a reduction in SOC content.

The HR was generally responsive to all the parameters related to soil microbial processes but in low sensitivity (Figure 7). The HR is widely affected by multiple abiotic and biotic conditions, such as substrate concentration, soil moisture, and soil temperature (Gomez-Casanovas et al., 2012; Zhang et al., 2013). In the CLM-Microbe model, HR is explicitly represented as soil microbial respiration under the influences of environmental factors (i.e., soil moisture, soil temperature, and oxygen concentration). Meanwhile, fungal and bacterial respiration is not only related to C gain through the decomposition of DOM, SOM, and litter and microbial DOM uptake, but also to soil microbial lysis (Figure 1). Therefore, HR is directly determined by the microbial activities and substrate availability, and indirectly affected by a wide range of environmental factors and parameters. For example, parameters defining C transfer from litter and SOM pools to fungal and bacterial biomass pools and DOM, from DOM pool to fungal and bacterial biomass and SOM pools, and from fungal and bacterial biomass pools to DOM and SOM pools are closely related to soil microbial C gain and loss.

In general, the CLM-Microbe model simulated comparable SOC and HR in grasslands, tundra, temperate broadleaf forests, tropical/subtropical forests, and wetlands, but much higher SOC and HR in shrub, boreal forests, and temperate coniferous forests compared with CLM4.5 (Table 5). This may be due to two reasons. First, to produce reasonable vegetation status, we adjusted the parameters related to plant photosynthesis (e.g., *flnr*) and C allocation (e.g., *froot_leaf*) in the CLM-Microbe model to guarantee reasonable vegetation productivity indicated by MODIS data set. However, when running the CLM4.5, we used the default parameters for each plant functional type. Therefore, the difference in vegetation condition may induce the discrepancy in simulated SOC and HR. For example, we documented a SOC pool of 2,568 g C m^{-2} and HR flux of 277 g C m^{-2} yr^{-1}, but both SOC and HR were zeros in desert site (DST-CH) because of vegetation mortality. Litterfall from vegetation serves as the C source for SOM formation (Thornton & Rosenbloom, 2005), the difference in vegetation condition may be one of the important reasons for the difference in simulated SOC and HR between CLM4.5 and the CLM-Microbe model. Second, to produce comparable SOC in the CLM-Microbe model with HSWD data set, we adjusted active soil depth for decomposition (*decomp_depth_efolding*) to reach the goal. While we used the default value of *decomp_depth_efolding* (0.5) for the CLM4.5 simulation in all sites. *decomp_depth_efolding* determines the vertical distribution of SOC in the soil profile, changes in *decomp_depth_efolding* may account for the differences in simulated SOC, and possibly HR, between CLM4.5 and the CLM-Microbe model (Bonan et al., 2013).

4.4. Limitations and Improvements

The CLM-Microbe model is capable of simulating FBC and BBC dynamics across biomes; a few improvements are identified as our future research needs. First, the dormant portion of fungi and bacteria were not explicitly considered in the CLM-Microbe model. Dormant soil microbes can become viable in short time periods due to their capability of rapidly sensing limiting resources change (Garcia-Pichel & Pringault, 2001). Therefore, dormant soil microbes are able to survive environmental stresses and serve as "seed banks" for the soil microbial community (Lennon & Jones, 2011). Representing the dormant portion of soil microbes would enhance the model capability in simulating microbial resilience to stressful conditions (G. Wang et al., 2015). Second, fresh C input-induced priming effects is an important pathway affecting microbial activity, which needs to be considered in future studies. In addition to environmental factors such as temperature, soil moisture, and oxygen concentration, the addition of organic or mineral substances available for soil microorganisms may stimulate microbial activities, causing priming effects (Blagodatskaya & Kuzyakov, 2008). However, we did not test the model performance in simulating the priming impact within

current model structure. Given the different physiology of bacteria and fungi, it would be worthwhile to robustly test the model behavior in simulating the priming effect, and further improve the model as needed.

Third, the soil food web regulates fungal and bacterial biomass dynamics, thus the inclusion of soil trophic interactions would help better understand the effects of soil food web on soil microbial biomass dynamics. Soil microbial growth is strongly shaped by predation, Buckeridge et al. (2013), for example, observed the seasonal variation in soil microbial community structure, and the decline in FBC from winter to late winter, and then again in spring, which was closely associated with the abundance of protozoa. Therefore, FBC and BBC may not only be controlled by abiotic factors such as soil temperature, soil moisture, oxygen concentration, and C availability, but the seasonal variation in their predator communities (Schadt et al., 2003). Fourth, the FBC and BBC data compiled were measured using a wide range of methods, while different methods may introduce a variety of biases (L. He et al., 2020). For example, direct microscopy was widely used in early stage of soil microbial studies, but the approach has inevitably included dead biomass of soil microbes, especially for fungi, into the estimated biomass (Buckeridge et al., 2013). Amino sugars such as glucosamine and muramic acid are used to estimate FBC and BBC, respectively; however, this method measures both living and dead microbial biomass due to the high stability of amino sugars in soil (Glaser et al., 2004). Therefore, comparing FBC and BBC data measured by multiple methods will suffer from uncertainties in data quality due to various biases introduced by the different methods. Although data-model integration has been proposed for more than four decades, the intimate collaboration between experimentalists and modelers is still needed for model development. A standardized microbial data system that contains primary microbial variables with consistent measurement approach or after conversion is critical to reduce the bias associated with distinct methods (Xu et al., 2020). Last but not least, the observed data for bacterial and fungal biomass C commonly vary by more than five orders of magnitude (Guo et al., 2020; L. He et al., 2020; Sinsabaugh et al., 2016; Xu et al., 2013, 2017), while ecosystem-level variables commonly vary by less than three orders of magnitude. This large discrepancy makes the validation approach applied to ecosystem-level C pools and fluxes less robust in microbial models, as shown in this study of model validation (Section 3.1). The CLM-Microbe is able to reasonably capture the seasonality of key microbial variables but less robust in simulating the magnitude of microbial variables. We call for community-level efforts to develop a new model validation approach that is more applicable to microbial models.

5. Conclusions

This study reported the model parameterization, validation, uncertainty analysis, and sensitivity analysis of the CLM-Microbe model in simulating fungal and bacterial biomass at the site level. The CLM-Microbe model could simulate the seasonal variation of FBC and BBC, but the model tended to underestimate the magnitude of the observed biomass for most biomes. Sensitivity analysis showed that the turnover rates of FBC and BBC are the most important parameters regulating FBC and BBC, respectively. Meanwhile, C flow from SOM to soil microbes during decomposition and the C:N ratio of fungal and bacterial biomass are also important for FBC and BBC dynamics. We observed an enhancement of soil microbial C gain from SOM on SOC, but the enhancement is weak in tundra and boreal forests. The simulated HR was responsive to all parameters related to soil microbial processes across biomes but exhibited low sensitivity.

The CLM-Microbe model represents the first attempt to simulate the soil microbial effects on C cycle by differentiating fungi and bacteria and their physiology in assimilating C in soils. Along with the emerging microbial macroecology (Xu et al., 2020), the improvements in modeling microbial mechanisms will likely bring more robust abilities to ESMs to better simulate and project the climate system. The explicit representation of soil microbial processes into the CLM-Microbe model will improve our mechanistic understanding of ecosystem-level C cycling and improve predictability of microbial community structure at regional to global scales, thereby reducing uncertainties in global C projection.

Data Availability Statement

The data used for model parameterization and validation are obtained in published literature that have been clearly cited in the Table 1 of the manuscript.

Acknowledgments
The authors are grateful to Dr. Yimei Huang from Northwest A&F University, and Drs. Qian Zhao and Weijun Shen from South China Botanical Garden, Chinese Academy of Sciences for providing the exact sampling date of fungal and bacterial biomass. We thank Dr. Jörg Rinklebe from University of Wuppertal for providing the time-series data of fungal and bacterial biomass data. Liyuan He thanks Dr. Fenghui Yuan for the discussion about sensitivity analysis. This study is partially supported by San Diego State University and the CSU Program for Education & Research in Biotechnology. Partial support for this work was provided by an Early Career Award through the U.S. Department of Energy (DOE) Biological and Environmental Research Program ORNL is managed by UT-Battelle, LLC, under contract DE-AC05-00OR22725 with the U.S. DOE. This manuscript has been authored by UT-Battelle, LLC, under contract no. DE-AC05-00OR22725 with the US Department of Energy (DOE). The US government retains and the publisher, by accepting the article for publication, acknowledges that the US government retains a nonexclusive, paid-up, irrevocable, worldwide license to publish or reproduce the published form of this manuscript, or allow others to do so, for US government purposes. DOE will provide public access to these results of federally sponsored research in accordance with the DOE Public Access Plan (http://energy.gov/downloads/doe-publicaccess-plan).

References

Aguilera, L. E., Armas, C., Cea, A. P., Gutiérrez, J. R., Meserve, P. L., & Kelt, D. A. (2016). Rainfall, microhabitat, and small mammals influence the abundance and distribution of soil microorganisms in a Chilean semi-arid shrubland. *Journal of Arid Environments*, *126*, 37–46. Retrieved from https://www.sciencedirect.com/science/article/pii/S0140196315300999

Allison, S. D. (2012). A trait-based approach for modelling microbial litter decomposition. *Ecology Letters*, *15*(9), 1058–1070. Retrieved from https://onlinelibrary.wiley.com/doi/full/10.1111/j.1461-0248.2012.01807.x

Allison, S. D., Wallenstein, M. D., & Bradford, M. A. (2010). Soil-carbon response to warming dependent on microbial physiology. *Nature Geoscience*, *3*(5), 336–340. Retrieved from https://www.nature.com/articles/ngeo846

Bailey, V. L., Peacock, A. D., Smith, J. L., & Bolton, H., Jr (2002). Relationships between soil microbial biomass determined by chloroform fumigation–extraction, substrate-induced respiration, and phospholipid fatty acid analysis. *Soil Biology and Biochemistry*, *34*(9), 1385–1389. Retrieved from https://www.sciencedirect.com/science/article/pii/S0038071702000706

Bai, Z., Xu, H. J., He, H. B., Zheng, L.C., & Zhang, X.-D. (2013). Alterations of microbial populations and composition in the rhizosphere and bulk soil as affected by residual acetochlor. *Environmental Science and Pollution Research*, *20*(1), 369–379. Retrieved from https://link.springer.com/article/10.1007/s11356-012-1061-3

Balser, T. C., Treseder, K. K., & Ekenler, M. (2005). Using lipid analysis and hyphal length to quantify AM and saprotrophic fungal abundance along a soil chronosequence. *Soil Biology and Biochemistry*, *37*(3), 601–604. Retrieved from https://www.sciencedirect.com/science/article/pii/S0038071704003116

Beare, M. H. (1997). Fungal and bacterial pathways of organic matter decomposition and nitrogen mineralization in arable soils. *Soil Ecology in Sustainable Agricultural Systems*, 37–70. Retrieved from https://agris.fao.org/agris-search/search.do?recordID=US1997058729

Bell, C. W., Tissue, D. T., Loik, M. E., Wallenstein, M. D., Martinez, V. A., Erickson, R. A., & Zak, J. C. (2014). Soil microbial and nutrient responses to 7 years of seasonally altered precipitation in a Chihuahuan Desert grassland. *Global Change Biology*, *20*(5), 1657–1673. Retrieved from https://onlinelibrary.wiley.com/doi/abs/10.1111/gcb.12418

Bittman, S., Forge, T. A., & Kowalenko, C. G. (2005). Responses of the bacterial and fungal biomass in a grassland soil to multi-year applications of dairy manure slurry and fertilizer. *Soil Biology and Biochemistry*, *37*(4), 613–623. Retrieved from https://www.sciencedirect.com/science/article/pii/S0038071704002913

Björk, R. G., Björkman, M. P., Andersson, M. X., & Klemedtsson, L. (2008). Temporal variation in soil microbial communities in Alpine tundra. *Soil Biology and Biochemistry*, *40*(1), 266–268. Retrieved from https://www.sciencedirect.com/science/article/pii/S0038071707003136

Björk, R. G., Klemedtsson, L., Molau, U., Harndorf, J., Ödman, A., & Giesler, R. (2007). Linkages between N turnover and plant community structure in a tundra landscape. *Plant and Soil*, *294*(1), 247–261. https://doi.org/10.1007/s11104-007-9250-4

Blagodatskaya, E., & Kuzyakov, Y. (2008). Mechanisms of real and apparent priming effects and their dependence on soil microbial biomass and community structure: Critical review. *Biology and Fertility of Soils*, *45*(2), 115–131. Retrieved from https://link.springer.com/article/10.1007/s00374-008-0334-y

Bonan, G., Drewniak, B., Huang, M., Koven, C. D., Levis, S., Li, F., et al. (2013). *Technical description of version 4.5 of the community land model (CLM)*. NCAR Techical Note NCAR/TN-503+ STR. Natl

Bradford, M. A., & Fierer, N. (2012). The biogeography of microbial communities and ecosystem processes: Implications for soil and ecosystem models. In D. H. Wall et al. (Eds.), Soil ecology and ecosystem services (Vol. 18). Oxford University Press.

Buckeridge, K. M., Banerjee, S., Siciliano, S. D., & Grogan, P. (2013). The seasonal pattern of soil microbial community structure in mesic low arctic tundra. *Soil Biology and Biochemistry*, *65*, 338–347. https://doi.org/10.1016/j.soilbio.2013.06.012

Burns, R. G., DeForest, J. L., Marxsen, J., Sinsabaugh, R. L., Stromberger, M. E., Wallenstein, M. D., et al. (2013). Soil enzymes in a changing environment: Current knowledge and future directions. *Soil Biology and Biochemistry*, *58*, 216–234. https://doi.org/10.1016/j.soilbio.2012.11.009

Carnell, R., & Carnell, M. R. (2019). *Package 'lhs'* (p. 780). Retrieved from https://github.com/bertcarnell/lhs, http://cran.stat.auckland.ac.nz/web/packages/lhs/lhs.pdf

Chapin, F. S., Matson, P. A., & Vitousek, P. (2011). *Principles of terrestrial ecosystem ecology*. Springer Science & Business Media.

Cherrier, J., Bauer, J., & Druffel, E. (1996). Utilization and turnover of labile dissolved organic matter by bacterial heterotrophs in eastern North Pacific surface waters. *Marine Ecology Progress Series*, *139*, 267–279. https://www.int-res.com/abstracts/meps/v139/p267-279/

Cleveland, C. C., Nemergut, D. R., Schmidt, S. K., & Townsend, A. R. (2007). Increases in soil respiration following labile carbon additions linked to rapid shifts in soil microbial community composition. *Biogeochemistry*, *82*(3), 229–240. https://doi.org/10.1007/s10533-006-9065-z

Cole, J. J. (1999). Aquatic microbiology for ecosystem scientists: New and recycled paradigms in ecological microbiology. *Ecosystems*, *2*(3), 215–225. https://doi.org/10.1007/s100219900069

CPD, B., R, R., Aam, N., Gc, C., H, W., Aj, K., et al. (1995). Effects of grazing, sedimentation and phytoplankton cell lysis on the structure of a coastal pelagic food web. *Marine Ecology Progress Series*, *123*, 259–271. Retrieved from https://www.int-res.com/abstracts/meps/v123/p259-271/

Davidson, E. A., & Janssens, I. A. (2006). Temperature sensitivity of soil carbon decomposition and feedbacks to climate change. *Nature*, *440*(7081), 165–173. Retrieved from https://www.nature.com/articles/nature04514

Davidson, E. A., Samanta, S., Caramori, S. S., & Savage, K. (2012). The Dual Arrhenius and Michaelis–Menten kinetics model for decomposition of soil organic matter at hourly to seasonal time scales. *Global Change Biology*, *18*(1), 371–384. Retrieved from https://onlinelibrary.wiley.com/doi/full/10.1111/j.1365-2486.2011.02546.x

Devêvre, O. C., & Horwáth, W. R. (2000). Decomposition of rice straw and microbial carbon use efficiency under different soil temperatures and moistures. *Soil Biology and Biochemistry*, *32*(11–12), 1773–1785. Retrieved from https://www.sciencedirect.com/science/article/pii/S0038071700000961

Devi, N. B., & Yadava, P. S. (2006). Seasonal dynamics in soil microbial biomass C, N and P in a mixed-oak forest ecosystem of Manipur, North-east India. *Applied Soil Ecology*, *31*(3), 220–227. Retrieved from https://www.sciencedirect.com/science/article/pii/S0929139305001058

Díaz-Raviña, M., Acea, M. J., & Carballas, T. (1995). Seasonal changes in microbial biomass and nutrient flush in forest soils. *Biology and Fertility of Soils*, *19*(2), 220–226. https://doi.org/10.1007/BF00336163

Docherty, K. M., Borton, H. M., Espinosa, N., Gebhardt, M., Gil-Loaiza, J., Gutknecht, J. L. M., et al. (2015). Key edaphic properties largely explain temporal and geographic variation in soil microbial communities across four biomes. *PLOS One*, *10*(11). Retrieved from https://www.ncbi.nlm.nih.gov/pmc/articles/PMC4633200/

Dornbush, M., Cambardella, C., Ingham, E., & Raich, J. (2008). A comparison of soil food webs beneath C_3- and C_4-dominated grasslands. *Biology and Fertility of Soils*, *45*(1), 73–81. https://doi.org/10.1007/s00374-008-0312-4

Fang, C., Smith, P., Smith, J. U., & Moncrieff, J. B. (2005). Incorporating microorganisms as decomposers into models to simulate soil organic matter decomposition. *Geoderma*, *129*(3), 139–146. Retrieved from https://www.sciencedirect.com/science/article/pii/S0016706104003581

Feng, W., Zou, X., & Schaefer, D. (2009). Above- and belowground carbon inputs affect seasonal variations of soil microbial biomass in a subtropical monsoon forest of southwest China. *Soil Biology and Biochemistry*, *41*(5), 978–983. Retrieved from https://www.sciencedirect.com/science/article/pii/S0038071708003453

Fierer, N., Allen, A. S., Schimel, J. P., & Holden, P. A. (2003). Controls on microbial CO_2 production: A comparison of surface and subsurface soil horizons. *Global Change Biology*, *9*(9), 1322–1332. Retrieved from https://onlinelibrary.wiley.com/doi/full/10.1046/j.1365-2486.2003.00663.x

Flanagan, P. W., & Van Cleve, K. (1977). Microbial biomass, respiration and nutrient cycling in a Black Spruce Taiga ecosystem. *Ecological Bulletins*, (25), 261–273. Retrieved from https://www.jstor.org/stable/20112588

Frostegård, A., & Bååth, E. (1996). The use of phospholipid fatty acid analysis to estimate bacterial and fungal biomass in soil. *Biology and Fertility of Soils*, *22*(1–2), 59–65. Retrieved from https://link.springer.com/article/10.1007/BF00384433

Garcia-Pichel, F., & Pringault, O. (2001). Cyanobacteria track water in desert soils. *Nature*, *413*(6854), 380–381. Retrieved from https://www.nature.com/articles/35096640/

Glaser, B., Turrión, M.-B., & Alef, K. (2004). Amino sugars and muramic acid—Biomarkers for soil microbial community structure analysis. *Soil Biology and Biochemistry*, *36*(3), 399–407. Retrieved from https://www.sciencedirect.com/science/article/pii/S0038071703003407

Gomez-Casanovas, N., Matamala, R., Cook, D. R., & Gonzalez-Meler, M. A. (2012). Net ecosystem exchange modifies the relationship between the autotrophic and heterotrophic components of soil respiration with abiotic factors in prairie grasslands. *Global Change Biology*, *18*(8), 2532–2545. Retrieved from https://onlinelibrary.wiley.com/doi/full/10.1111/j.1365-2486.2012.02721.x

Gommers, P. J. F., Schie, B. J. v., Dijken, J. P. v., & Kuenen, J. G. (1988). Biochemical limits to microbial growth yields: An analysis of mixed substrate utilization. *Biotechnology and Bioengineering*, *32*(1), 86–94. Retrieved from https://onlinelibrary.wiley.com/doi/abs/10.1002/bit.260320112

Göttlicher, S. G., Steinmann, K., Betson, N. R., & Högberg, P. (2006). The dependence of soil microbial activity on recent photosynthate from trees. *Plant and Soil*, *287*(1–2), 85–94. Retrieved from https://link.springer.com/article/10.1007/s11104-006-0062-8

Gougoulias, C., Clark, J. M., & Shaw, L. J. (2014). The role of soil microbes in the global carbon cycle: Tracking the below-ground microbial processing of plant-derived carbon for manipulating carbon dynamics in agricultural systems. *Journal of the Science of Food and Agriculture*, *94*(12), 2362–2371. Retrieved from https://www.onlinelibrary.wiley.com/doi/abs/10.1002/jsfa.6577

Gruber, N., & Galloway, J. N. (2008). An Earth-system perspective of the global nitrogen cycle. *Nature*, *451*(7176), 293–296. Retrieved from https://www.nature.com/articles/nature06592?draft=journal

Gu, Z., Eils, R., & Schlesner, M. (2016). Complex heatmaps reveal patterns and correlations in multidimensional genomic data. *Bioinformatics*, *32*(18), 2847–2849. Retrieved from https://academic.oup.com/bioinformatics/article/32/18/2847/1743594

Guo, Z., Wang, Y., Wan, Z., Zuo, Y., He, L., Li, D., et al. (2020). Soil dissolved organic carbon in terrestrial ecosystems: Global budget, spatial distribution and controls. *Global Ecology and Biogeography*. Retrieved from https://onlinelibrary.wiley.com/doi/full/10.1111/geb.13186

Haefner, J. W. (2005). *Modeling biological systems-principles and applications*. New York, NY: Springer.

He, L., Rodrigues, J. L. M., Soudzilovskaia, N. A., Barceló, M., Olsson, P. A., Song, C., et al. (2020). Global biogeography of fungal and bacterial biomass carbon in topsoil. *Soil Biology and Biochemistry*, 108024. Retrieved from https://www.sciencedirect.com/science/article/pii/S0038071720303205

He, Y., Yang, J., Zhuang, Q., Harden, J. W., McGuire, A. D., Liu, Y., et al. (2015). Incorporating microbial dormancy dynamics into soil decomposition models to improve quantification of soil carbon dynamics of northern temperate forests. *Journal of Geophysical Research: Biogeosciences*, *120*(12), 2596–2611. Retrieved from https://agupubs.onlinelibrary.wiley.com/doi/abs/10.1002/2015JG003130

Hopkins, D. W., Sparrow, A. D., Elberling, B., Gregorich, E. G., Novis, P. M., Greenfield, L. G., & Tilston, E. L. (2006). Carbon, nitrogen and temperature controls on microbial activity in soils from an Antarctic dry valley. *Soil Biology and Biochemistry*, *38*(10), 3130–3140. Retrieved from https://www.sciencedirect.com/science/article/pii/S0038071706000940

Huang, G., Li, Y., & Su, Y. G. (2015). Effects of increasing precipitation on soil microbial community composition and soil respiration in a temperate desert, Northwestern China. *Soil Biology and Biochemistry*, *83*, 52–56. Retrieved from https://www.sciencedirect.com/science/article/pii/S003807171500019X

Ingham, E. R., Trofymow, J. A., Ames, R. N., Hunt, H. W., Morley, C. R., Moore, J. C., & Coleman, D. C. (1986). Trophic interactions and nitrogen cycling in a semi-arid grassland soil. I. Seasonal dynamics of the natural populations, their interactions and effects on nitrogen cycling. *Journal of Applied Ecology*, *23*(2), 597–614. Retrieved from https://www.jstor.org/stable/2404039

Jobbágy, E. G., & Jackson, R. B. (2000). The vertical distribution of soil organic carbon and its relation to climate and vegetation. *Ecological Applications*, *10*(2), 423–436. https://doi.org/10.1890/1051-0761(2000)010[0423:TVDOSO]2.0.CO;2

Kaiser, C., Koranda, M., Kitzler, B., Fuchslueger, L., Schnecker, J., Schweiger, P., et al. (2010). Belowground carbon allocation by trees drives seasonal patterns of extracellular enzyme activities by altering microbial community composition in a beech forest soil. *New Phytologist*, *187*(3), 843–858. https://doi.org/10.1111/j.1469-8137.2010.03321.x

Keohane, R. O. (2015). The global politics of climate change: Challenge for political science. *PS: Political Science & Politics*, *48*(1), 19–26. https://doi.org/10.1017/S1049096514001541

Kirchman, D. L., Suzuki, Y., Garside, C., & Ducklow, H. W. (1991). High turnover rates of dissolved organic carbon during a spring phytoplankton bloom. *Nature*, *352*(6336), 612–614. Retrieved from https://www.nature.com/articles/352612a0

Klamer, M., & Bååth, E. (2004). Estimation of conversion factors for fungal biomass determination in compost using ergosterol and PLFA 18: 2ω6, 9. *Soil Biology and Biochemistry*, *36*(1), 57–65. https://doi.org/10.1016/j.soilbio.2003.08.019

Koven, C. D., Riley, W. J., Subin, Z. M., Tang, J. Y., Torn, M. S., Collins, W. D., et al. (2013). The effect of vertically resolved soil biogeochemistry and alternate soil C and N models on C dynamics of CLM4. *Biogeosciences*, *10*(11), 7109. Retrieved from https://bg.copernicus.org/articles/10/7109/2013/

Landesman, W. J., & Dighton, J. (2010). Response of soil microbial communities and the production of plant-available nitrogen to a two-year rainfall manipulation in the New Jersey Pinelands. *Soil Biology and Biochemistry*, *42*(10), 1751–1758. https://doi.org/10.1016/j.soilbio.2010.06.012

Larionova, A. A., Yevdokimov, I. V., & Bykhovets, S. S. (2007). Temperature response of soil respiration is dependent on concentration of readily decomposable C. *Biogeosciences*, *4*(6), 1073–1081. Retrieved from https://hal.archives-ouvertes.fr/hal-00297658/

Lennon, J. T., & Jones, S. E. (2011). Microbial seed banks: The ecological and evolutionary implications of dormancy. *Nature Reviews Microbiology*, *9*(2), 119–130. Retrieved from https://www.nature.com/articles/nrmicro2504

Liang, C., Amelung, W., Lehmann, J., & Kästner, M. (2019). Quantitative assessment of microbial necromass contribution to soil organic matter. *Global Change Biology*, *25*(11), 3578–3590. Retrieved from https://onlinelibrary.wiley.com/doi/abs/10.1111/gcb.14781

Lipson, D. A., Schadt, C. W., & Schmidt, S. K. (2002). Changes in soil microbial community structure and function in an alpine dry meadow following spring snow melt. *Microbial Ecology*, *43*(3), 307–314. Retrieved from https://link.springer.com/article/10.1007%2Fs00248-001-1057-x?LI=true

Lipson, D. A., & Schmidt, S. K. (2004). Seasonal changes in an alpine soil bacterial community in the Colorado Rocky Mountains. *Applied and Environmental Microbiology*, *70*(5), 2867–2879. Retrieved from https://aem.asm.org/content/70/5/2867

Liu, D., Huang, Y., Yan, H., Jiang, Y., Zhao, T., & An, S. (2018). Dynamics of soil nitrogen fractions and their relationship with soil microbial communities in two forest species of northern China. *PLoS One*, *13*(5). Retrieved from https://www.ncbi.nlm.nih.gov/pmc/articles/PMC5967799/

Luo, Y., Keenan, T. F., & Smith, M. (2015). Predictability of the terrestrial carbon cycle. *Global Change Biology*, *21*(5), 1737–1751. Retrieved from https://onlinelibrary.wiley.com/doi/full/10.1111/gcb.12766

Miura, T., Makoto, K., Niwa, S., Kaneko, N., & Sakamoto, K. (2017). Comparison of fatty acid methyl ester methods for characterization of microbial communities in forest and arable soil: Phospholipid fraction (PLFA) versus total ester linked fatty acids (EL-FAME). *Pedobiologia*, *63*, 14–18. Retrieved from https://www.sciencedirect.com/science/article/pii/S0031405616301652

Moche, M., Gutknecht, J., Schulz, E., Langer, U., & Rinklebe, J. (2015). Monthly dynamics of microbial community structure and their controlling factors in three floodplain soils. *Soil Biology and Biochemistry*, *90*, 169–178. https://doi.org/10.1016/j.soilbio.2015.07.006

Moore, J. C., McCann, K., & de Ruiter, P. C. (2005). Modeling trophic pathways, nutrient cycling, and dynamic stability in soils. *Pedobiologia*, *49*(6), 499–510. Retrieved from https://www.sciencedirect.com/science/article/pii/S0031405605000545

National Ecological Observatory Network. (2020). *Data product DP1.10104.001, soil microbe biomass*. Boulder, CO: USA NEON. Retrieved from http://data.neonscience.orgon

Olsson, P. a. A., & Wallander, H. a. (1998). Interactions between ectomycorrhizal fungi and the bacterial community in soils amended with various primary minerals. *FEMS Microbiology Ecology*, *27*(2), 195–205. Retrieved from https://academic.oup.com/femsec/article/27/2/195/531512

Paul, E. A. (2016). The nature and dynamics of soil organic matter: Plant inputs, microbial transformations, and organic matter stabilization. *Soil Biology and Biochemistry*, *98*, 109–126. https://doi.org/10.1016/j.soilbio.2016.04.001

Peters, G. P., Andrew, R. M., Boden, T., Canadell, J. G., Ciais, P., Le Quéré, C., et al. (2012). The challenge to keep global warming below 2°C. *Nature Climate Change*, *3*, 4–6. Retrieved from https://www.nature.com/articles/nclimate1783

Priha, O., Grayston, S. J., Pennanen, T., & Smolander, A. (1999). Microbial activities related to C and N cycling and microbial community structure in the rhizospheres of Pinus sylvestris, Picea abies and Betula pendula seedlings in an organic and mineral soil. *FEMS Microbiology Ecology*, *30*(2), 187–199. Retrieved from https://academic.oup.com/femsec/article/30/2/187/609507?view=extract

Pritchard, S. G., Strand, A. E., McCormack, M. L., Davis, M. A., & Oren, R. (2008). Mycorrhizal and rhizomorph dynamics in a loblolly pine forest during 5 years of free-air-CO_2-enrichment. *Global Change Biology*, *14*(6), 1252–1264. Retrieved from https://onlinelibrary.wiley.com/doi/abs/10.1111/j.1365-2486.2008.01567.x

Rousk, J., & Bååth, E. (2007). Fungal biomass production and turnover in soil estimated using the acetate-in-ergosterol technique. *Soil Biology and Biochemistry*, *39*(8), 2173–2177. https://doi.org/10.1016/j.soilbio.2007.03.023

Rousk, J., & Bååth, E. (2011). Growth of saprotrophic fungi and bacteria in soil. *FEMS Microbiology Ecology*, *78*(1), 17–30. https://doi.org/10.1111/j.1574-6941.2011.01106.x

Schadt, C. W., Martin, A. P., Lipson, D. A., & Schmidt, S. K. (2003). Seasonal dynamics of previously unknown fungal lineages in tundra soils. *Science*, *301*(5638), 1359–1361. Retrieved from https://science.sciencemag.org/content/301/5638/1359

Schimel, J. P., & Weintraub, M. N. (2003). The implications of exoenzyme activity on microbial carbon and nitrogen limitation in soil: A theoretical model. *Soil Biology and Biochemistry*, *35*(4), 549–563. https://doi.org/10.1016/S0038-0717(03)00015-4

Schindlbacher, A., Rodler, A., Kuffner, M., Kitzler, B., Sessitsch, A., & Zechmeister-Boltenstern, S. (2011). Experimental warming effects on the microbial community of a temperate mountain forest soil. *Soil Biology and Biochemistry*, *43*(7), 1417–1425. https://doi.org/10.1016/j.soilbio.2011.03.005

Schippers, A., Neretin, L. N., Kallmeyer, J., Ferdelman, T. G., Cragg, B. A., John Parkes, R., & Jørgensen, B. B. (2005). Prokaryotic cells of the deep sub-seafloor biosphere identified as living bacteria. *Nature*, *433*(7028), 861–864. Retrieved from https://www.nature.com/articles/nature03302

Schmidt, S. K., Costello, E. K., Nemergut, D. R., Cleveland, C. C., Reed, S. C., Weintraub, M. N., et al. (2007). Biogeochemical consequences of rapid microbial turnover and seasonal succession in soil. *Ecology*, *88*(6), 1379–1385. Retrieved from https://esajournals.onlinelibrary.wiley.com/doi/abs/10.1890/06-0164

Sinsabaugh, R. L., Manzoni, S., Moorhead, D. L., & Richter, A. (2013). Carbon use efficiency of microbial communities: Stoichiometry, methodology and modelling. *Ecology Letters*, *16*(7), 930–939. Retrieved from https://onlinelibrary.wiley.com/doi/full/10.1111/ele.12113

Sinsabaugh, R. L., Turner, B. L., Talbot, J. M., Waring, B. G., Powers, J. S., Kuske, C. R., et al. (2016). Stoichiometry of microbial carbon use efficiency in soils. *Ecological Monographs*, *86*(2), 172–189. Retrieved from https://esajournals.onlinelibrary.wiley.com/doi/abs/10.1890/15-2110.1

Sistla, S. A., Rastetter, E. B., & Schimel, J. P. (2014). Responses of a tundra system to warming using SCAMPS: A stoichiometrically coupled, acclimating microbe–plant–soil model. *Ecological Monographs*, *84*(1), 151–170. Retrieved from https://esajournals.onlinelibrary.wiley.com/doi/full/10.1890/12-2119.1

Six, J., Frey, S. D., Thiet, R. K., & Batten, K. M. (2006). Bacterial and fungal contributions to carbon sequestration in agroecosystems. *Soil Science Society of America Journal*, *70*(2), 555–569. Retrieved from https://acsess.onlinelibrary.wiley.com/doi/abs/10.2136/sssaj2004.0347

Spohn, M. (2015). Microbial respiration per unit microbial biomass depends on soil litter carbon-to-nitrogen ratio. *Biogeosciences*, *12*, 817–823. Retrieved from https://eref.uni-bayreuth.de/17270/

Stahl, P. D., & Parkin, T. B. (1996). Relationship of soil ergosterol concentration and fungal biomass. *Soil Biology and Biochemistry*, *28*(7), 847–855. Retrieved from https://www.sciencedirect.com/science/article/pii/0038071796000612

Strickland, M. S., & Rousk, J. (2010). Considering fungal: Bacterial dominance in soils–methods, controls, and ecosystem implications. *Soil Biology and Biochemistry*, *42*(9), 1385–1395. Retrieved from https://www.sciencedirect.com/science/article/pii/S0038071710001689

Sulman, B. N., Phillips, R. P., Oishi, A. C., Shevliakova, E., & Pacala, S. W. (2014). Microbe-driven turnover offsets mineral-mediated storage of soil carbon under elevated CO_2. *Nature Climate Change*, *4*(12), 1099–1102. Retrieved from https://www.nature.com/articles/nclimate2436

Tang, J., & Riley, W. J. (2015). Weaker soil carbon–climate feedbacks resulting from microbial and abiotic interactions. *Nature Climate Change*, *5*(1), 56–60. Retrieved from https://www.nature.com/articles/nclimate2438

Taylor, K. E., Stouffer, R. J., & Meehl, G. A. (2011). An overview of CMIP5 and the experiment design. *Bulletin of the American Meteorological Society*, *93*(4), 485–498. Retrieved from https://journals.ametsoc.org/doi/abs/10.1175/BAMS-D-11-00094.1

Thornton, P. E., Lamarque, J.-F., Rosenbloom, N. A., & Mahowald, N. M. (2007). Influence of carbon-nitrogen cycle coupling on land model response to CO_2 fertilization and climate variability. *Global Biogeochemical Cycles*, *21*(4). Retrieved from https://agupubs.onlinelibrary.wiley.com/doi/full/10.1029/2006GB002868

Thornton, P. E., & Rosenbloom, N. A. (2005). Ecosystem model spin-up: Estimating steady state conditions in a coupled terrestrial carbon and nitrogen cycle model. *Ecological Modelling*, *189*(1–2), 25–48. Retrieved from https://www.sciencedirect.com/science/article/pii/S0304380005001948

Treseder, K. K., Balser, T. C., Bradford, M. A., Brodie, E. L., Dubinsky, E. A., Eviner, V. T., et al. (2012). Integrating microbial ecology into ecosystem models: Challenges and priorities. *Biogeochemistry*, *109*(1), 7–18. https://doi.org/10.1007/s10533-011-9636-5

Van Der Heijden, M. G. A., Bardgett, R. D., & Van Straalen, N. M. (2018). The unseen majority: Soil microbes as drivers of plant diversity and productivity in terrestrial ecosystems. *Ecology Letters*, 296–310. https://doi.org/10.1111/j.1461-0248.2007.01139.x

von Lützow, M., & Kögel-Knabner, I. (2009). Temperature sensitivity of soil organic matter decomposition—What do we know? *Biology and Fertility of Soils*, *46*(1), 1–15. Retrieved from https://link.springer.com/article/10.1007/s00374-009-0413-8

Wallander, H. A., Göransson, H., & Rosengren, U. (2004). Production, standing biomass and natural abundance of ^{15} N and ^{13} C in ectomycorrhizal mycelia collected at different soil depths in two forest types. *Oecologia*, *139*(1), 89–97. Retrieved from https://link.springer.com/article/10.1007/s00442-003-1477-z

Wang, G., Jagadamma, S., Mayes, M. A., Schadt, C. W., Steinweg, J. M., Gu, L., & Post, W. M. (2015). Microbial dormancy improves development and experimental validation of ecosystem model. *The ISME Journal*, *9*(1), 226–237. Retrieved from https://www.nature.com/articles/ismej2014120

Wang, G., Post, W. M., & Mayes, M. A. (2013). Development of microbial-enzyme-mediated decomposition model parameters through steady-state and dynamic analyses. *Ecological Applications*, *23*(1), 255–272. Retrieved from https://esajournals.onlinelibrary.wiley.com/doi/full/10.1890/12-0681.1

Wang, K., Peng, C., Zhu, Q., Zhou, X., Wang, M., Zhang, K., & Wang, G. (2017). Modeling global soil carbon and soil microbial carbon by integrating microbial processes into the ecosystem process model TRIPLEX-GHG. *Journal of Advances in Modeling Earth Systems*, *9*(6), 2368–2384. Retrieved from https://agupubs.onlinelibrary.wiley.com/doi/abs/10.1002/2017MS000920

Wang, Y., Yuan, F., Yuan, F., Gu, B., Hahn, M. S., Torn, M. S., et al. (2019). Mechanistic modeling of microtopographic impacts on CO_2 and CH_4 Fluxes in an Alaskan tundra ecosystem using the CLM-Microbe model. *Journal of Advances in Modeling Earth Systems*, *11*, 17. Retrieved from https://agupubs.onlinelibrary.wiley.com/doi/full/10.1029/2019MS001771

Waring, B. G., Averill, C., & Hawkes, C. V. (2013). Differences in fungal and bacterial physiology alter soil carbon and nitrogen cycling: Insights from meta-analysis and theoretical models. *Ecology Letters*, *16*(7), 887–894.

Wheeler, P. A., Gosselin, M., Sherr, E., Thibaultc, D., Kirchman, D. L., Benner, R., & Whitledge, T. E. (1996). Active cycling of organic carbon in the central Arctic Ocean. *Nature*, *380*(6576), 697–699. Retrieved from https://www.nature.com/articles/380697a0

Wieder, W. R., Allison, S. D., Davidson, E. A., Georgiou, K., Hararuk, O., He, Y., et al. (2015). Explicitly representing soil microbial processes in Earth system models. *Global Biogeochemical Cycles*, *29*(10), 1782–1800. Retrieved from https://agupubs.onlinelibrary.wiley.com/doi/abs/10.1002/2015GB005188

Wieder, W. R., Bonan, G. B., & Allison, S. D. (2013). Global soil carbon projections are improved by modelling microbial processes. *Nature Climate Change*, *3*(10), 909–912. Retrieved from https://www.nature.com/articles/nclimate1951

Wieder, W. R., Grandy, A. S., Kallenbach, C. M., & Bonan, G. B. (2014). Integrating microbial physiology and physio-chemical principles in soils with the MIcrobial-MIneral Carbon Stabilization (MIMICS) model. *Biogeosciences*, *11*(14), 3899–3917. Retrieved from https://www.biogeosciences.net/11/3899/2014/

Xiao, Y. (2003). Variation in needle longevity of Pinus tabulaeformis forests at different geographic scales. *Tree Physiology*, *23*(7), 463–471. Retrieved from https://academic.oup.com/treephys/article/23/7/463/1665446

Xu, X. (2010). *Modeling methane and nitrous oxide exchanges between the atmosphere and terrestrial ecosystems over North America in the context of multifactor global change* (Ph.D. Dissertation). Auburn, AL: Auburn University.

Xu, X., Elias, D. A., Graham, D. E., Phelps, T. J., Carroll, S. L., Wullschleger, S. D., & Thornton, P. E. (2015). A microbial functional group-based module for simulating methane production and consumption: Application to an incubated permafrost soil. *Journal of Geophysical Research: Biogeosciences*, *120*(7), 1315–1333. Retrieved from https://agupubs.onlinelibrary.wiley.com/doi/abs/10.1002/2015JG002935

Xu, X., Schimel, J. P., Janssens, I. A., Song, X., Song, C., Yu, G., et al. (2017). Global pattern and controls of soil microbial metabolic quotient. *Ecological Monographs*, *87*(3), 429–441. Retrieved from https://esajournals.onlinelibrary.wiley.com/doi/full/10.1002/ecm.1258

Xu, X., Schimel, J. P., Thornton, P. E., Song, X., Yuan, F., & Goswami, S. (2014). Substrate and environmental controls on microbial assimilation of soil organic carbon: A framework for Earth system models. *Ecology Letters*, *17*(5), 547–555. https://doi.org/10.1111/ele.12254

Xu, X., Thornton, P. E., & Post, W. M. (2013). A global analysis of soil microbial biomass carbon, nitrogen and phosphorus in terrestrial ecosystems. *Global Ecology and Biogeography*, *22*(6), 737–749. https://doi.org/10.1111/geb.12029.

Xu, X., Wang, N., Lipson, D., Sinsabaugh, R., Schimel, J., He, L., et al. (2020). Microbial macroecology: In search of mechanisms governing microbial biogeographical patterns. *Global Ecology and Biogeography*. https://doi.org/10.1111/geb.13162

Yuste, J. C., Peñuelas, J., Estiarte, M., Garcia-Mas, J., Mattana, S., Ogaya, R., et al. (2011). Drought-resistant fungi control soil organic matter decomposition and its response to temperature. *Global Change Biology*, *17*(3), 1475–1486. Retrieved from https://onlinelibrary.wiley.com/doi/abs/10.1111/j.1365-2486.2010.02300.x

Zaehle, S., Friend, A. D., Friedlingstein, P., Dentener, F., Peylin, P., & Schulz, M. (2010). Carbon and nitrogen cycle dynamics in the O-CN land surface model: 2. Role of the nitrogen cycle in the historical terrestrial carbon balance. *Global Biogeochemical ssCycles*, *24*(1). Retrieved from https://agupubs.onlinelibrary.wiley.com/doi/abs/10.1029/2009GB003522

Zhang, Q., Lei, H.-M., & Yang, D.-W. (2013). Seasonal variations in soil respiration, heterotrophic respiration and autotrophic respiration of a wheat and maize rotation cropland in the North China Plain. *Agricultural and Forest Meteorology*, *180*, 34–43. Retrieved from https://www.sciencedirect.com/science/article/pii/S0168192313001056

Zhao, Q., Jian, S., Nunan, N., Maestre, F. T., Tedersoo, L., He, J., et al. (2017). Altered precipitation seasonality impacts the dominant fungal but rare bacterial taxa in subtropical forest soils. *Biology and Fertility of Soils*, *53*(2), 231–245. https://doi.org/10.1007/s00374-016-1171-z